Solubilization and stabilization of membrane proteins by cycloalkane-modified amphiphilic polymers.

Anaïs Marconnet, Baptiste Michon, Christel Le Bon, Fabrice Giusti, Christophe Tribet, Manuela Zoonens

Solubilization and stabilization of membrane proteins by cycloalkane-modified amphiphilic polymers.

Anaïs Marconnet,[1,2] Baptiste Michon,[1,2] Christel Le Bon,[1,2] Fabrice Giusti,[1,2,†] Christophe Tribet,[3,] Manuela Zoonens[1,2,]**

[1]Université de Paris, Laboratoire de Biologie Physico-Chimique des Protéines Membranaires, CNRS, UMR 7099, F-75005 Paris, France. [2]Institut de Biologie Physico-Chimique, Fondation Edmond de Rothschild pour le développement de la recherche Scientifique, F-75005 Paris, France. [3]P.A.S.T.E.U.R., Département de Chimie, École Normale Supérieure, PSL University, Sorbonne Université, CNRS, F-75005 Paris, France.

KEYWORDS: amphipols, extraction, membrane proteins, SMA co-polymers, stability, surfactants.

ABSTRACT: Membrane proteins need to be extracted from biological membranes and purified in their native state for most structural and functional *in vitro* investigations. Amphiphilic copolymers, such as amphipols (APols), have emerged as very useful alternatives to detergents for keeping membrane proteins water-soluble under their native form. However, classical APols, *i.e.* poly(acrylic acid) (PAA) derivatives, seldom enable direct membrane protein extraction. Poly(styrene-maleic anhydride) copolymers (SMAs), which bear aromatic rings as hydrophobic side groups, have been reported to be more effective extracting agents. In order to test the hypothesis of a role of cyclic hydrophobic moieties in membrane solubilization by copolymers, we have prepared PAA derivatives comprising cyclic rather than linear aliphatic side groups (CyclAPols). As references, APol A8-35, SMAs, and diisobutylene maleic acid (DIBMA) were compared with CyclAPols. Using as models the plasma membrane of *Escherichia coli* and the extraction-resistant purple membrane from *Halobacterium salinarum*, we show that CyclAPols combine the extraction efficiency of SMAs with the stabilization afforded to membrane proteins by classical APols such as A8-35.

Introduction

As gatekeepers of all membrane compartments in cells, membrane proteins (MPs) fulfill essential biological functions and are key targets for drugs.[1,2] Their importance motivates structural and biophysical studies, which, however, critically depend on extraction/purification procedures that keep MPs in their native state. Detergents can disrupt biological membranes and keep MPs water-soluble, but they often entail MP inactivation, in part due to their propensity to detach from MPs endogenous lipids or cofactors needed for activity. This has prompted the development of macromolecular amphiphiles such as amphipols (APols),[3–5] which were expected to be less aggressive dispersing agents and less prone to reach hidden hydrophobic regions in the protein. The prototypical APol, named A8-35, is a poly(acrylic acid) (PAA) polymer randomly modified with octylamine and isopropylamine side chains (Figure 1A). The mildness of APol association with MPs results in an increased life-time of the native state of APol-complexed MPs.[5] Another advantage of APols is the improvement of images in the fast growing field of single-particle electron cryo-microscopy (cryo-EM) reconstitution.[5,6] Conventional APols are however poor solubilizing agents for biological membranes, by far less efficient than most detergents.[7,8] They can break liposomes (lacking MPs),[9–11] but in practice MP/APol complexes can rarely be directly obtained from biological membranes and must be prepared by transferring the protein from detergent-solubilized extracts.[5,12] Styrene maleic acid (SMA) co-polymers (Figure 1B) are APol variants with the distinctive property of enabling direct dispersion of proteolipidic membranes with no need for detergent.[13,14] They form lipid-protein-polymer mixed nanodiscs, called SMALPs. Spontaneous formation of lipid nanodiscs is not specific to SMAs as it has been observed with lipids and diisobutylene/maleic acid copolymers (DIBMA, Figure 1C)[15] and with copolymers similar to APols.[16] Despite several limitations such as high UV absorbance, due to the presence of aromatic groups, and polydispersity of the discs,[17] the use

of SMAs has developed in the field of MPs thanks to their solubilizing property. However, in the field of structural biology, the frequent need to use harsh extraction conditions may explain the low number of high-resolution cryo-EM structures established using SMAs.[6,18] To date, only a small number of single-particle cryo-EM structures of SMALPs have been obtained.[6] In comparison, despite the need for surfactant exchange, classical APols (mainly A8-35 and PMAL-C8)[3,19,20] represent the most frequently used polymers.[6] To circumvent the need of surfactant exchange, improving the direct solubilization of membranes by APol-like polymers under mild experimental conditions would be highly desirable.

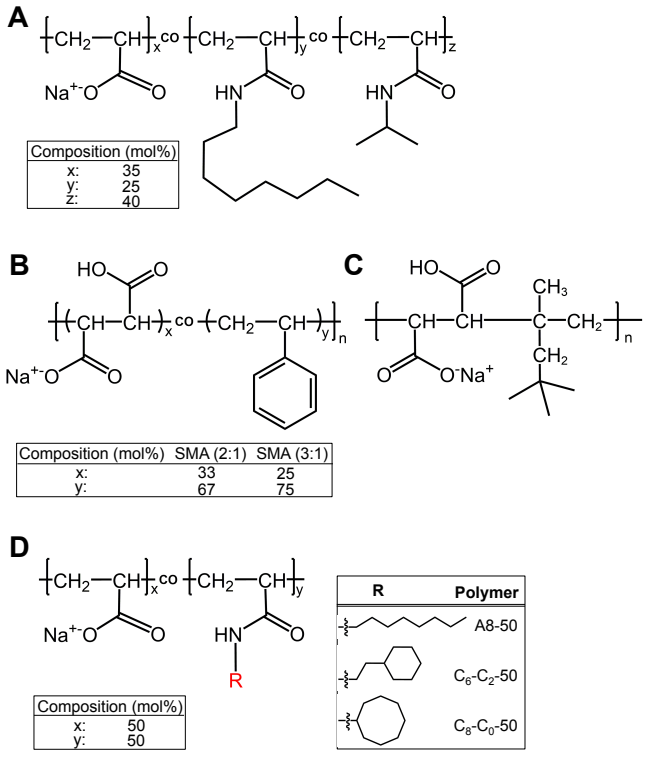

Figure 1. Chemical structures of amphipathic polymers used in this study. A) A8-35; molar percentages of each unit are from ref.[3] B) SMA co-polymers, with molar ratios of styrene to maleic acid units of 2:1 or 3:1 ($n \approx 9$).[15] C) DIBMA co-polymer ($n \approx 37$).[15] D) PAA modified with either linear or cyclic hydrocarbon groups (R) of 8 carbon atoms. The $\overline{M}_n$ values for C_6-C_2-50, C_8-C_0-50 and A8-50 (sodium salt form) were calculated using $\overline{DP}_n \approx 35$ for the parent PAA[21] and the degree of grafting, *y*, determined by ^{13}C, ^{1}H NMR and potentiometric titration

(~53 ± 1, ~51 ± 3, and ~56 ± 4 mol% for C_6-C_2-50, C_8-C_0-50 and A8-50, respectively; see Figures S1 to S7 in SI and Table 1).

We hypothesized that replacing the flexible *n*-alkyl side groups of classical APols by cyclic hydrophobic groups might possibly mimic the role of SMA's aromatic side groups. Of note, introducing cyclic groups in the aliphatic tail of dodecylmaltoside results in MP-stabilizing analogs.[22] We therefore examined whether cyclic hydrocarbon groups grafted onto PAA might not *i)* improve the polymers' ability to break up MP-containing membranes while *ii)* preserving the long-term stability of MPs. To this end, we prepared copolymers, named CyclAPols, in which the linear octyl groups of A8-35-like APols were replaced by cyclic ones having the same number of carbon atoms (either cyclohexylethylamine or cyclooctylamine, yielding polymers C_6-C_2-50 and C_8-C_0-50, respectively, Figure 1D). Cycloalkanes were preferred over aromatic cycles in order to keep the CyclAPols UV-transparent. As references, we compared CyclAPols with SMA (2:1) and (3:1) of relatively short length,[14,23,24] DIBMA, and polyacrylate-based APols with linear side groups, namely A8-35 and A8-50 (an APol possessing a density of hydrophobic moieties of ~50%, *i.e.* equal to that of SMA (2:1) and CyclAPols).

We studied the membrane-solubilizing properties of CyclAPols using as a model the plasma membrane of *Escherichia coli*, a host cell widely used for producing recombinant MPs.[25,26] We expressed two different MPs, YidC of *E. coli* fused to a green fluorescent protein (GFP), and the bacteriorhodopsin of *Haloquadratum walsbyi* (*Hw*BR). To further examine the solubilizing properties of CyclAPols, we used the native purple membrane from *Halobacterium salinarum*, which is well known for its resistance to solubilization by polymers, be they SMA[13,27] or classical APols.[5] Finally, the thermal stability of BR from *Hb. salinarum* (*Hs*BR) extracted with various APols was evaluated.

Experimental Section

1) Chemicals

DIBMA and *n*-Dodecyl β-D-maltoside (DDM) were supplied by Anatrace. As indicated by the supplier, DIBMA was a purified version of Sokalan CP9 from BASF. SMA (2:1) and SMA (3:1) were obtained from ProFoldin (SMA21S) and Polyscope (Xiran SL25010 P20), respectively. The number-average molecular masses ($\overline{M}_n$) of DIBMA and SMA (3:1) co-polymers were ~8,400 g·mol^{-1} and ~4,000 g·mol^{-1}, respectively.[15] The lipid 1,2-dimyristoyl-sn-glycero-3-phosphocholine (DMPC) was purchased from Avanti Polar Lipids.

2) Synthesis of APols and composition determination

The synthesis of A8-35 was performed as previously reported.[3] APol derivatives carrying either octylamine, cyclohexylethylamine or cyclooctylamine were obtained after a single step of poly(acrylic acid) (PAA) modification. Briefly, the hydrophobic side chains were randomly grafted onto PAA of $\overline{M}_w$~ 5.5 kDa in *N*-methylpyrrolidone (NMP) in the presence of dicyclohexylcarbodiimide (DCC). In each case, the resulting polymer obtained under the acidic form was purified by four cycles of precipitation/solubilization in water, performed at acidic and basic pH, respectively. The final polymer solution adjusted at pH 8-9 was dialyzed against MilliQ water and freeze-dried, yielding the expected APol. After synthesis, the final yields of APols were 98% and 96% for CyclAPols C_6-C_2-50 and C_8-C_0-50, respectively, and 86% and 52% for APols of reference A8-35 and A8-50, respectively.

The grafting ratio of hydrophobic side chains was determined by ^{13}C and ^{1}H NMR spectroscopy (Figures S1 to S6) and potentiometric titration in a water/ethanol mixture (20:80, v/v) (Figure S7). The ^{13}C NMR spectra of polymers, at 100 g·L^{-1} in deuterated methanol, were obtained after a long acquisition time (48-60h) due to the long delay between

each frequency pulse required for a complete relaxation of all carbon nuclei. The average degree of polymerization ($\overline{DP}_n$) of the commercial PAA used in this study for synthesizing A8-35 and the APol derivatives was previously determined to be close to ~35 by size exclusion chromatography (SEC) analysis in organic solvent.[21] The number-average molar masses ($\overline{M}_n$) of sodium salts of APol derivatives were calculated with the $\overline{DP}_n$ value and the grafting ratio (y) averaged from ^{13}C and ^{1}H NMR spectroscopy and pH-titration determination (Table 1).

APol	**CO_2^- (x_1/x_2, %)**	**Hydrophobic groups (y_1/y_2, %)**	***x* (%)**	***y* (%)**	**$\overline{M}_n$ (g·mol^{-1})**
C_6-C_2-50	47/46	53/54	46.5 ± 0.5	53.5 ± 0.5	4919
C_8-C_0-50	52/46	48/54	49 ± 3	51 ± 3	4843
A8-50	47/40	53/60	43.5 ± 3.5	56.5 ± 3.5	5050

Table 1. Chemical compositions and number-average molecular masses of polyacrylate-based APols. The percentages of grafts and free carboxylates were deduced from an average of ^{1}H and ^{13}C NMR analysis (yielding y_1 and x_1) and from acid-base titrations (yielding y_2 and x_2) for each APol. The values were averaged, giving the final x and y ratios. For the APol of reference A8-35, the averaged final ratios were x = 34%, y = 23% and z = 43%, and the $\overline{M}_n$ value was 4276 g·mol^{-1}.

3) Expression of YidC-GFP of E. coli *and BR of* Hq. walsbyi *in* E. coli *strain and quantification of protein extraction using polymers*

The expression vectors encoding for YidC of *E. coli* fused at its C-terminus to GFP (YidC-GFP) and BR of *Hq. walsbyi* (*Hw*BR) were kindly provided by the laboratories of Jan Whilem and Anant Menon, respectively. The strains *E. coli* C41 and C43 (DE3) were transformed with each vector, respectively, and growth at 37°C in LB in the presence of either ampicillin or kanamycin. When the optical density at 600 nm reached 0.6-0.8, the cultures

were supplemented with IPTG. In the case of *Hw*BR production, 5 µM all-*trans* retinal (Sigma) were also added. After induction, cells were harvested. The pellet of each culture was re-suspended with buffer containing 20 mM Tris-HCl, 150 mM NaCl, pH 8.0 and cell lysis was performed with a Cell Disruptor (Constant Systems). Unbroken cells and cellular debris were removed by centrifugation (20 min. at 10,000 × *g*). The membranes were harvested from supernatants by high-speed centrifugation (1h at 100,000 × *g*). The concentration of total MPs present in the membrane extracts was assessed with a calorimetric assay.

The solubilization of YidC-GFP from *E. coli* membranes was performed at a total MP concentration of 2 $g \cdot L^{-1}$ with either 1% w/v DDM, used as reference condition, or 2 $g \cdot L^{-1}$ polymers, corresponding to a total MP/polymer ratio of 1:1 (w/w). After 1 h incubation at 4°C, the samples were centrifuged 30 min. at 100,000 × *g*. The supernatants and the pellets, re-suspended in the initial volume of solubilization with buffer 20 mM Tris-HCl, 150 mM NaCl, pH 8.0 and 5% SDS, were loaded on 12-% acrylamide gels. After migration, the gels were washed with water and the fluorescence of GFP within the gel was detected with a Typhoon TLA 9500 (GE healthcare). The excitation and emission wavelengths were those of Alexa Fluor 488, *i.e.* 495 nm and 519 nm, respectively. The fluorescence of the band corresponding to YidC-GFP visible on the acrylamide gels was quantified using Image J software. The fluorescence of YidC-GFP measured for each supernatant was normalized with the fluorescence quantified for the 1%-DDM supernatant, which was defined as the maximum of solubilization. For the kinetic of YidC-GFP extraction, the solubilization was performed under the same experimental conditions except that aliquots taken off from samples were centrifuged 10 min. at 250,000 × *g*.

In the case of *Hw*BR, the solubilization was carried out with both pure *E. coli* membranes and after the fusion of *E. coli* membranes with 100-nm extruded DMPC liposomes, prepared in 20 mM Tris-HCl, 150 mM NaCl, pH 8.0, by sonication in the dark for 30 min. using a bath

sonicator (VWR). The total MP/DMPC ratio was 1:0.5 (w/w), as previously reported.[28] The membranes were then supplemented with either 0.2% w/v DDM or polymers at a final concentration of 2 g·L^{-1}, *i.e.* a total MP/polymer ratio of 1:1 (w/w). After incubation for 4 h at room temperature, the samples were centrifuged 30 min. at 100,000 × *g* and *Hw*BR present in the supernatants was assessed with absorbance at 554 nm.

4) Quantification of native BR extracted from DMPC-fused purple membrane by polymers

The purple membrane was purified from *Hb. salinarum* as described.[29] The concentration of native BR of *Hb. salinarum* (*Hs*BR) was adjusted to 5 g·L^{-1} with buffer 20 mM sodium phosphate, 100 mM NaCl, pH 7.0 and the membrane preparation was stored at -80 °C until usage.

Fusion of the native purple membrane with DMPC liposomes was performed as reported.[13,27] Briefly, an aliquot of purple membrane was mixed with 100-nm extruded DMPC liposomes to reach a final *Hs*BR/DMPC ratio varying from 1:3 to 1:6 (w/w). The samples, at a *Hs*BR concentration of 0.5 g·L^{-1}, were sonicated in the dark for 30 min. using a bath sonicator (VWR) and then stored at -80°C until usage.

Solubilization was initiated by mixing at a 1:1 volume ratio DMPC-fused purple membrane with polymer solutions to reach a final *Hs*BR/polymer ratio varying from 1:3 to 1:9 (w/w). The samples were incubated overnight in the dark, at 25°C under shaking in a thermomixer. After an overnight incubation, all the samples were centrifuged at 4 °C for 20 min. at 200,000 × *g*. The UV-visible spectra of supernatants were recorded with a spectrophotometer (Hewlett Packard). The quantification of extracted *Hs*BR was evaluated with the ratio of absorbance values at 554 nm measured before and after centrifugation.

Because APols and SMAs are polydisperse polymers, the representation of the molar ratios of *Hs*BR/macromolecular chains depends on the weighted average of polymers mass. Here, we used the number averaged experimental values of $\overline{M}_n$. For *Hs*BR/polymer weight ratios of 1:3 and 1:9 (w/w), the corresponding molar ratios of *Hs*BR/C_8-C_0-50 are then of ~1:16.7 and ~1:50.3, respectively. For SMA (3:1), the average molar ratios of *Hs*BR/SMA correspond to ~1:20.3 and ~1:60.8, respectively. At (w/w) *Hs*BR/DMPC ratio fixed to 1:5, the (w/w) *Hs*BR/polymer ratios of 1:3 and 1:9 correspond in addition to molar ratios of DMPC/cycloalkane (from C_8-C_0-50) of ~1:1.6 and ~1:4.9, respectively. For SMA (3:1), the molar ratios of DMPC/phenyl rings was similarly of ~1:2.8 and ~1:8.3, respectively.

5) *Dynamic light scattering (DLS)*

The scattering intensity was measured at 25°C and an angle of 90° in a BI-200SM Brookhaven Instrument system equipped with a 30 mW 637 nm laser and photomultiplier detection. Size distributions from all samples showed a monomodal distribution as analyzed by CONTIN. Hydrodynamic diameters (D_H) were calculated by fitting the correlation functions by the cumulant analysis method at quadratic order. For the kinetics of solubilization, a sample of DMPC-fused purple membrane (at 0.2 $g{\cdot}L^{-1}$ of *Hs*BR) was mixed with a polymer solution (1:1 v/v) to reach a final *Hs*BR/polymer ratio of 1:12.5 (w/w).

6) Size exclusion chromatography (SEC)

The solution dispersity of *Hs*BR/DMPC/polymer complexes was characterized by SEC. After *Hs*BR extraction, the samples were injected onto a Superose 12 10/300 GL column connected to an Äkta purifier-10 system (GE Healthcare). The sample and elution buffer was

20 mM sodium phosphate, 100 mM NaCl, pH 7.0. Elution was carried out at room temperature and UV absorbance monitored at three wavelengths (220, 280 and 554 nm).

7) Stability assay

Samples of *Hs*BR (extracted directly from DMPC-fused purple membrane with polymers) were incubated at 50°C for 6h in the dark in a thermomixer. UV-visible spectra of samples were recorded each hour. The decrease of the absorbance value at 554 nm reflects the loss of retinal and a change in the native conformation of the protein. The absorbance values were normalized with the initial one, *i.e.* measured at 4°C.

Results

1. Synthesis of CyclAPols

The synthesis of the CyclAPol derivatives consists in the random grafting on a PAA backbone of cycloalkane moieties *via* the formation of amide bonds. The average degree of grafting was controlled quantitatively by introduction of *ad hoc* percentages of cycloalkylamine reactants to reach values similar to the hydrophobic moieties in SMA (2:1), *i.e.* 50 mol% (within experimental error). The average percentages of grafting of cyclohexylethylamine and cyclooctylamine, yielding C_6-C_2-50 and C_8-C_0-50, respectively, were then determined by both ^{13}C and ^{1}H NMR spectroscopy and pH titration (Table 1). The resulting CyclAPols were highly soluble in aqueous solutions and UV-transparent (Figure S8).

The solubilizing properties of CyclAPols, assessed with biological membranes from two different origins, were compared with a set of five other polymers used as references: *i)* the commercially-available polymers SMA (2:1) and (3:1), which both carry cyclic aromatic rings as hydrophobic moieties with a density of 50 and 67 mol%, respectively, *ii)* the commercially-available polymer DIBMA, which carries short-length branched acyclic side groups present along the polymer at 33 mol%, and *iii)* the polyacrylate-based APols A8-35 and A8-50, which carry linear octyl chains grafted at 25 and 50 mol%, respectively. In contrast to A8-50, the archetypical APol A8-35 also comprises isopropyl moieties at 40 mol%, whose role is to reduce its charge density. The number-average molar masses ($\overline{M}_n$) of CyclAPol derivatives, A8-50, A8-35, and SMA (3:1) are comparable. In term of dispersity, CyclAPols, A8-50 and A8-35 were derived from the same PAA parent chain and, as a result, have the same polydispersity ($Đ \approx 2.0$), whereas the polydispersity of SMAs is slightly

broader (typically 2.0-2.5).[23] Regarding DIBMA, its $\bar{M}_n$ value is larger and its polydispersity slightly narrower ($Đ \approx 1.8$)[30] than that of the other copolymers used in this study.

2. *Solubilization by CyclAPols of* E. coli *plasma membrane fragments*

The solubilizing properties of CyclAPols were tested with membrane fragments from *E. coli*. Two different MPs were expressed and used as target MPs to estimate the extraction efficiency of each polymer. The first protein was YidC of *E. coli*, an insertase whose transmembrane domain comprises six α-helices.[31] A version of YidC fused at its C-terminus with GFP (YidC-GFP) was used as reporter to quantify the solubilization yields. In Figure 2 are reported the amounts of polymer-extracted YidC-GFP recovered in the supernatants after 1 hour of incubation at 4°C at a fixed total MP/polymer ratio of 1:1 (w/w). Under these experimental conditions, the yields of YidC-GFP extracted with CyclAPols were the highest as compared to the references, *i.e.* A8-35, A8-50, the two SMAs and DIBMA (Figure 2A). The amounts of CyclAPol-extracted YidC-GFP were almost twice that obtained with A8-50 (~70-75% *vs.* ~40%). Monitoring the solubilization over 2-h incubation of the membranes with CyclAPols revealed a rapid increase of YidC-GFP fluorescence in supernatants before reaching a plateau after ~45 min. (Figure 2B). A 1-h incubation suffices to reach the maximal extraction (Figure 2A), whereas extraction by either one of the two SMAs or by A8-35 progresses more slowly (Figure 2B).

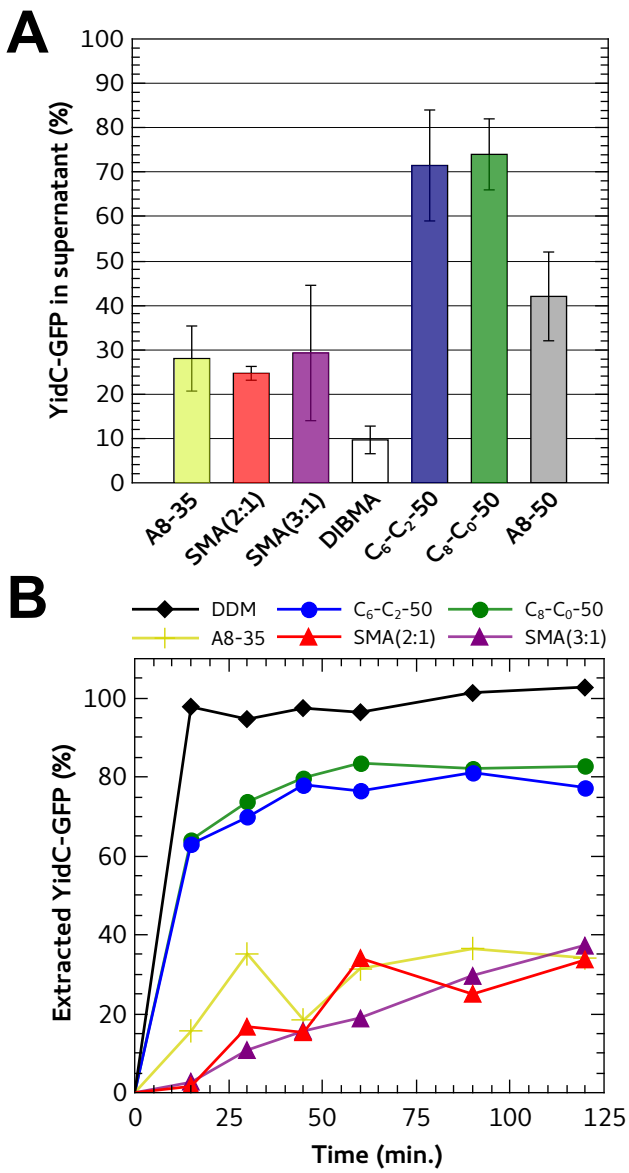

Figure 2. Fraction of YidC-GFP extracted from *E. coli* membranes upon addition of different polymers. A) Quantification of YidC-GFP extracted from *E. coli* membranes. Membranes were supplemented with each polymer stock solution to reach a final polymer concentration of 2 g·L^{-1} (*i.e.* a total MP/polymer (w/w) ratio of 1:1) and incubated for 1 h at 4°C. The buffer contained 20 mM Tris-HCl, 150 mM NaCl, pH 8.0. After centrifugation (30 min. at 100,000 × *g*), the protein content in the supernatants was analyzed by SDS-PAGE. The in-gel detection of YidC-GFP fluorescence was quantified with ImageJ. The fluorescence intensity of polymer-extracted YidC-GFP was normalized to the fluorescence intensity for YidC-GFP

solubilized with 1% w/v (10 g·L^{-1}) DDM, used as reference for a complete extraction. B) Kinetics of YidC-GFP extraction from *E. coli* membranes after addition of polymers. Over 2 h of incubation, aliquots were taken off from each sample and centrifuged (10 min. at 250,000 × *g*). The fluorescence of the supernatants was quantified in gel (Figure S9).

The second MP expressed in *E. coli* and used as reporter was the archaebacterial bacteriorhodopsin of *Hq. walsbyi* (*Hw*BR) produced under its native conformation as indicated by its spectroscopic signature. This protein is a light-driven proton pump, whose transmembrane domain folds in a bundle of 7 α-helices.[32] The amounts of *Hw*BR extracted with A8-35 and SMA (2:1) were the lowest (Figure 3). In contrast to observations with YidC-GFP, the results obtained with *Hw*BR revealed significant differences between A8-35 and the two SMAs. SMA (3:1) appeared to be more efficient at extracting *Hw*BR from *E. coli* membranes than either SMA (2:1) or A8-35 (Figure 3). When solubilizing *E. coli* membranes with CyclAPols, the amounts of extracted *Hw*BR were 2.5× higher than with SMA (3:1). As previously reported, the solubilization efficiency of SMA (3:1) can be improved by modulating the bilayer characteristics with the addition of synthetic phospholipids DMPC.[28] This treatment increased the amount of SMA (3:1)-solubilized *Hw*BR (+50%), which remains nevertheless below the amount extracted by CyclAPols (Figure 3B). Intriguingly, no significant differences between CyclAPols and A8-50 were noted, in contrast to observations with YidC-GFP. Kinetics of solubilization over 4-h incubation of the *E. coli* membranes with polymers revealed that the maximal extraction of *Hw*BR in CyclAPol-containing supernatants was reached in 1h, whereas extraction by SMA (3:1) progressed more slowly (Figure S10).

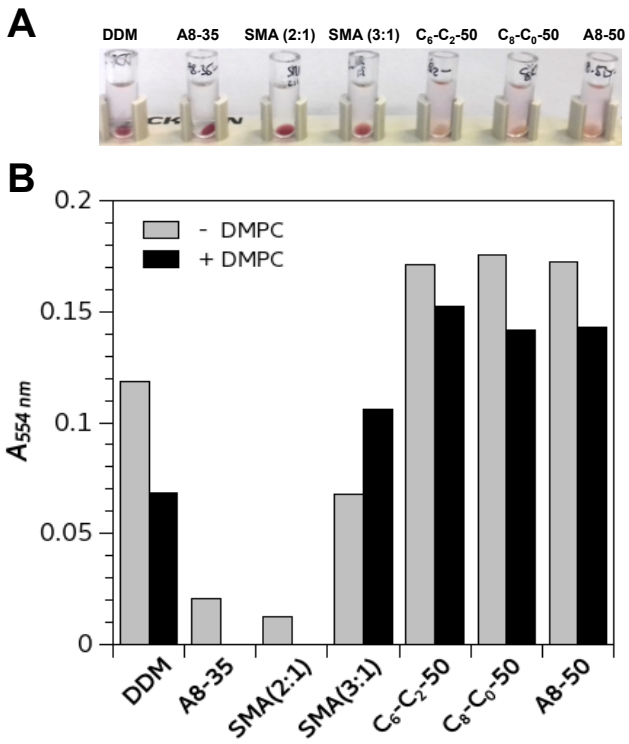

Figure 3. Extraction of *Hq. walsbyi* BR (*Hw*BR) from *E. coli* membranes using various surfactants. The solubilization of *E. coli* membranes was carried out at room temperature at a final polymer concentration of 2 g·L^{-1}, corresponding to a total MP/polymer ratio of 1:1 (w/w). The reference condition in the presence of detergent was carried out with 0.2% w/v (2 g·L^{-1}) DDM. The buffer was 20 mM Tris-HCl, 150 mM NaCl, pH 8.0. After 4 h, the samples were centrifuged (30 min. at 100,000 × *g*) and the concentration of *Hw*BR in the supernatants quantified by measuring the absorbance at 554 nm. The same experiment was performed with *E. coli* membranes fused with DMPC at a total MP/DMPC ratio of 1:0.5 (w/w) as described in ref.[28] In the case of A8-35 and SMA (2:1), the absorbance values at 554 nm measured for supernatants collected after solubilization of DMPC-fused *E. coli* membranes were equal to 0.

3. Solubilization by CyclAPols of the purple membrane of Hb. salinarum

To further investigate the membrane-solubilizing capacities of CyclAPols, we tested them on the purple membrane from *Hb. salinarum*, which represents both a simpler model than *E. coli* membrane fragments, as it contains a single protein (*Hs*BR), and a demanding one because of the high density and tight packing of proteins (*Hs*BR is accounting for three quarters of the membrane mass).[29] Indeed, purple membrane fragments proved resistant to solubilization by all of the polymers tested. Dilution of *Hs*BR by fusion of the fragments with DMPC lipids was thus used to lower this resistance to solubilization.[13,27] In order to be able to rank the polymers according to their solubilization efficiency, solubilization was assessed at various *Hs*BR/DMPC ratios (Figure 4). A smaller pellet (Figure 4A) and higher recovery of native *Hs*BR in supernatants (Figure 4B) indicated that SMA (3:1) was by far more efficient at extracting *Hs*BR than SMA (2:1) and DIBMA (Figure S11). Under the same experimental conditions, A8-35 was unable to extract *Hs*BR, confirming its poor detergency. Even the more hydrophobic A8-50, which differs from A8-35 by a two-fold higher density of *n*-octyl chains, did not perform better than SMA (2:1). In contrast, CyclAPols, with a similar degree of grafted side groups as A8-50, were efficient solubilizers. The amounts of native *Hs*BR found in CyclAPol- and SMA (3:1)-containing supernatants were comparable (~80-85%). As expected, a decrease of extraction efficacy by SMAs was observed when lowering the DMPC content in proteoliposomes. In contrast, high percentages of solubilization were obtained with CyclAPols even at the lowest DMPC ratio, *i.e.* in the more demanding conditions (Figure 4B).

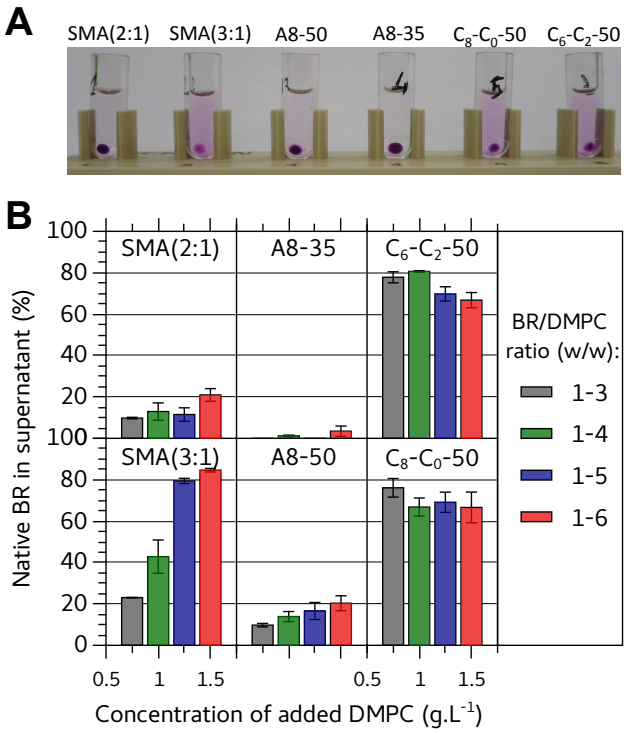

Figure 4. Solubilization by copolymers of DMPC-fused purple membrane at *Hs*BR/polymer ratio of 1:6.25 (w/w) upon varying the amount of added DMPC. DMPC-containing proteo-liposomes were prepared by fusion between DMPC liposomes and purple membrane diluted at 0.5 g·L^{-1} [*Hs*BR] (see Experimental section) before being mixed with an equal volume of polymer solution. Samples were incubated overnight at 25°C in the dark and then ultracentrifuged (20 min. at 200,000 × *g*). *A)* Photographs of samples after centrifugation (*Hs*BR/DMPC ratio = 1:5 w/w). B) Percentage of native *Hs*BR in the supernatants as quantified by the ratios of absorbance values at 554 nm measured before and after centrifugation.

To compare further CyclAPols and SMA (3:1), we assessed the effect of polymer concentration on the DMPC-fused purple membrane (at a fixed *Hs*BR/DMPC ratio of 1:5 w/w) and measured the size of the complexes formed in supernatants. The percentage of native,

solubilized *Hs*BR decreased sharply at low polymer concentration (Figure 5), indicating that a polymer/*Hs*BR ratio of 3:1 (w/w) is not sufficient to fully disperse all of the *Hs*BR. All three copolymers however enabled up to 90% solubilization at higher polymer/*Hs*BR ratios. Surprisingly, the amount of SMA (3:1)-solubilized *Hs*BR passed through a maximum, which is confirmed by the size of the purple pellets (Figure S12). The hydrodynamic diameter (D_H) of the complexes (at a *Hs*BR/polymer ratio of 1:6.25) were measured by DLS. Compared to SMA (3:1), the D_H of complexes formed with CyclAPols were smaller. The population of solubilized objects was also analyzed by size exclusion chromatography (SEC), confirming that *Hs*BR/DMPC/SMA (3:1) supernatants contained larger objects than those formed with CyclAPols (more material eluted in the void volume of the column; Figure S13). Therefore, whereas CyclAPols and SMA (3:1) can solubilize up to 90% *Hs*BR, the complexes formed with CyclAPols appear smaller and more monodisperse.

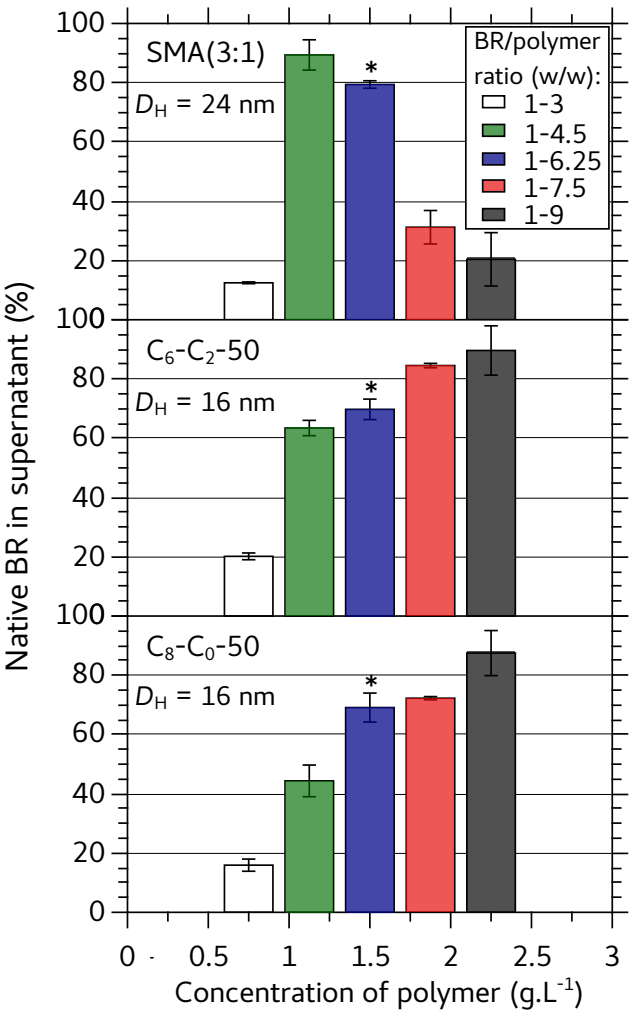

Figure 5. Fraction of native *Hs*BR extracted as a function of polymer concentration. The *Hs*BR/DMPC ratio was 1:5 (w/w) and the extraction procedure as described in the legend to Figure 4. Asterisks point to samples used for D_H measurement in supernatants by DLS at 25°C.

Next we assessed whether the copolymers solubilized the lipids along with *Hs*BR. To this aim, kinetics were recorded by DLS at a *Hs*BR/polymer ratio of 1:12.5 w/w (Figure 6). The scattered intensity reflects mainly evolution of proteoliposome size and concentration, because the small particles (free polymer particles and MP/polymer complexes; D_H < 40 nm) contribute less than 6% of the intensity. The scattered intensity typically decreased

immediately after supplementation of the *Hs*BR/DMPC proteoliposomes with a solution of polymer (1:1 v/v, see Experimental section), and gradually reached a plateau (in < 60 min. in the slowest case, that of A8-50). First, this kinetics validates that the 24-h incubation used to quantify the amount of solubilized *Hs*BR was sufficient to reach maximal extraction. Second, the average D_H as measured by DLS did not vary significantly with time and was about 130-200 nm (Table S1). This indicates that the proteoliposomes were the predominant scatterers during the whole solubilization. The absence of size variation, while the total intensity dropped down by up to 90%, rules out a gradual extraction of lipids or *Hs*BR from all membranes, and is thus incompatible with the "cookie-cutter" model proposed for SMAs.[33] In contrast, it is the number of proteoliposomes that decreases, without affecting the mean diameter of the residual ones. This probably indicates that once a liposome is destabilized (possibly due to the polymer gaining access to its internal surface), it rapidly disperses into small particles rather than undergoing a progressive size decrease. Interestingly, the plateau measured at long times correlates with the percentage of solubilized *Hs*BR. Namely, the plateau reached with A8-35 was the highest, revealing that ~80% of the initial proteoliposomes were left intact. In the presence of efficient solubilizers, either SMA (3:1) or CyclAPols, the scattered intensity decreased by up to 90%, which can be compared with the 90% *Hs*BR solubilization in Figures 4 and 5.

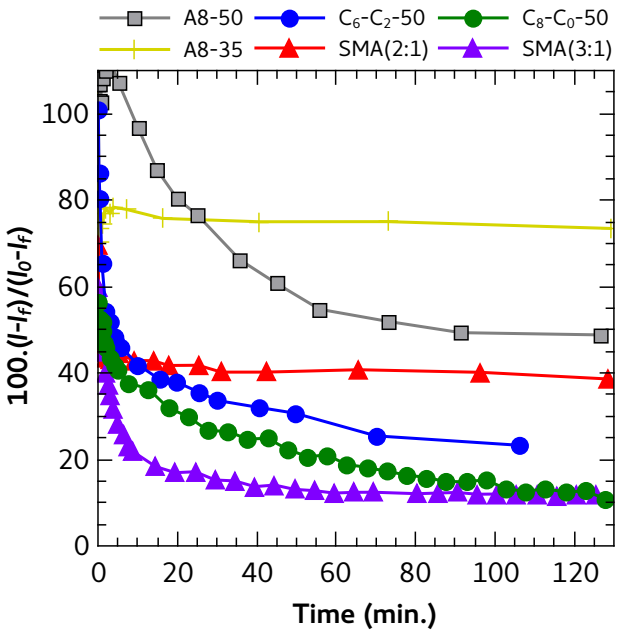

Figure 6. Kinetics of disruption of DMPC/purple membrane proteoliposomes upon addition of various polymers. At time 0, one volume of polymer solution was mixed to one volume of proteoliposomes. Kinetics were monitored at 25°C by measuring the light scattering intensity, *I*, at 90° angle (I_0 is the initial intensity and I_f the intensity scattered by supernatants 24 h after adding the polymers). The w/w ratios of *Hs*BR/DMPC and *Hs*BR/polymer were 1:5 and 1:12.5, respectively.

4. *Stability of CyclAPol-extracted* Hs*BR*

*Hs*BR carries a retinal chromophore whose spectroscopic properties are extremely sensitive to the conformation of its binding pocket.[34] Accordingly, the stability of *Hs*BR was assessed by measuring its absorbance at 554 nm. The kinetics of degradation were accelerated by incubating the complexes at 50°C. As shown in Figure 7, a rapid decrease of the fraction of native *Hs*BR is observed for SMA (3:1), whereas the spectral properties of *Hs*BR are stable for hours in CyclAPol-solubilized samples.

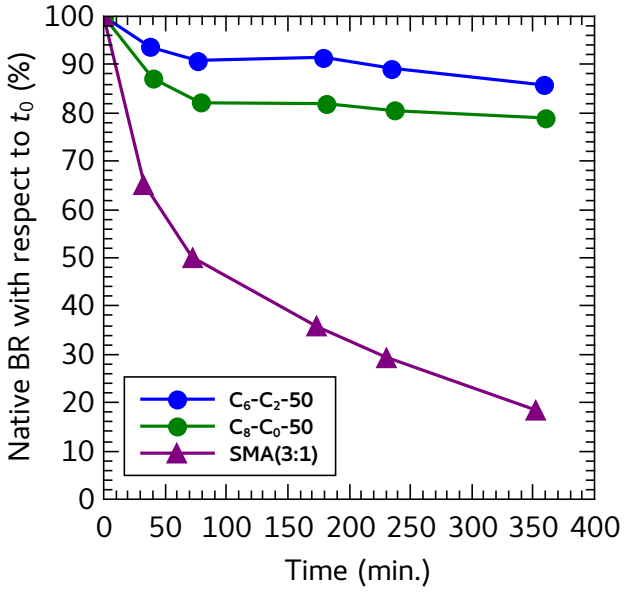

Figure 7. Kinetics of inactivation of *Hs*BR incubated at 50°C after extraction from DMPC-fused purple membrane with polymers. The (w/w) ratios of *Hs*BR/DMPC and *Hs*BR/polymer were 1:5 and 1:6.25, respectively. The rate of inactivation in SMA (2:1) is similar to that in SMA (3:1) but, because they bear on very small amounts, the data have not been plotted here.

Discussion

Detergent-free extraction of MPs using amphipathic polymers presents two main interests for structural and functional investigations of MPs. First, it avoids exposing the protein to detergent, which is a frequent cause of inactivation. Second, it increases the probability that the protein will retain lipids that are important to its function and stability. Among amphipathic polymers that can substitute for detergents, classical, polyacrylate-based APols (the prototype of which is A8-35) and SMA co-polymers are the most frequently used.[4,5,14] Classical APols like A8-35 are very mild surfactants, so that MPs must generally be first extracted with detergents before being transferred to the polymer.[12] SMAs present the advantage of being more solubilizing, so that direct MP extraction is often possible.[14] In the present study, improving the efficiency of polyacrylate-based APols at extracting MPs directly from membranes while preserving their stabilizing effect was attempted using newly designed APols carrying cycloalkane moieties (CyclAPols).

Although pure lipid liposomes can be dispersed with a comparable efficiency in the presence of many copolymers, such as A8-35, SMA (2:1) and CyclAPols (see Figure S14), this does not reflect their efficiency at extracting MPs. Biological membranes are indeed more complex systems than pure liposomes and the proteins to be extracted differ one from another. In the present study, the archaebacterial BR from two different organisms, that of *Hb. salinarum* naturally present in the purple membrane and that of *Hq. walsbyi* produced as a recombinant protein in *E. coli* were used as target protein to assess the efficiency of polymers at solubilizing MPs. The two BRs share 56% sequence identity, their transmembrane domain adopts the same fold, *i.e.* a bundle of 7 α-helices, and they bind the same cofactor, retinal, which, when bound to the native protein, gives BR its spectroscopic signature. By looking at the conditions required to extract the highest amounts of the two BR versions from their

respective membranes, *i.e.* the densely packed purple membrane and the more fluid *E. coli* membranes, the solubilizing properties of the polymers appear very similar. For instance, the efficiency of A8-35, SMA (2:1) and DIBMA at extracting BR is very limited regardless of the membrane used, whereas that of SMA (3:1) improves in the presence of exogenous lipids. The predominant lipid components of the plasma membrane of *E. coli* are the zwitterionic lipid phosphatidylethanolamine (75%) and the anionic lipids phosphatidylglycerol (20%) and cardiolipin.[35] By fusing DMPC, a zwitterionic lipid, the overall charges of the membrane decreases and the fluidity of the membrane is modified. These parameters presumably affect the efficiency of SMA (3:1) at extracting *Hw*BR. Under the same experimental conditions, *i.e.* at low polymer concentrations, CyclAPols show better capacities to extract *Hw*BR than either A8-35, SMA (2:1) or SMA (3:1). In addition, solubilization by CyclAPols is not as dependent on the addition of exogenous lipids as that by SMA (3:1) is. When the reporter protein is YidC-GFP, the protein-extraction efficiency of CyclAPols remains high, which suggests that the solubilizing properties of CyclAPols may be protein-independent. Recovering the highest amount of MPs *i)* at low polymer concentrations over a short period of incubation (typically 1 h) and *ii)* without the need to add exogenous lipids presents two advantages. First, it minimizes the risk of disruption of fragile interactions in MP complexes (amphipathic polymers, despite their lower dissociating character as compared to detergents, can also be disruptive when used at high concentrations).[5,36,37] Second, the natural lipid composition in the vicinity of the MP to be extracted is not modified.

The comparison of CyclAPols with their counterpart A8-50 highlights the importance of the cyclic nature of the hydrophobic moieties. A8-50 and the two CyclAPols have the same density of hydrophilic and hydrophobic moieties, *i.e.* ~50 mol%. However, A8-50, which comprises linear aliphatic (octyl) tails, allows one to recover lower amounts of both *Hs*BR from DMPC-fused purple membrane and YidC-GFP from *E. coli* membrane as compared to

CyclAPols. The comparison of CyclAPols with DIBMA, which carries ~33 mol% of acyclic short-length branched (diisobutyl), also shows a more efficient extraction with CyclAPols. The improvement of solubilization achieved with CyclAPols is therefore due to the cyclic nature of the hydrophobic side-groups. In the case of detergents, the few available data suggest that cyclic hydrophobic groups markedly affect their solution behavior.[38–40] In-tail cycles restrict packing possibilities, which is reflected in a lower propensity to self-assemble (up to 8 times higher critical micelle concentration compared to linear counterparts, lower aggregation number, more hydrated core).[38–40] A lower stability of intra-polymer hydrophobic association in CyclAPols likely makes these groups more available to interact with lipid bilayers, and thus to extract MPs. But other molecular parameters may also play a role. Not surprisingly, a higher density of hydrophobic side-groups in amphiphilic copolymers enhance their interaction with liposomes,[9,10] which is in line with their relative efficiency at solubilizing BR (SMA (2:1) < SMA (3:1) and A8-35 < A8-50). Overall, however, the density of side groups does not suffice to account for solubilization efficiency. Thus, the density of hydrophobic moieties along C_8-C_0-50 (or C_6-C_2-50) is the same as in A8-50, whereas these polymers exhibit significant differences in extraction efficiency (C_8-C_0-50 >> A8-50). Moreover, because cycloalkyl moieties expose less surface to water than linear chains, cyclic side groups are effectively less hydrophobic than linear ones, so that CyclAPols rank below A8-50 in term of effective hydrophobicity and could be expected to be less efficient solubilizers. A second possibly relevant parameter is the degree of ionization of the copolymer chains.[10] As APols are weak acids, ionization of polymer chains is reported to lower the detergency by markedly increasing hydrophilicity. Potentiometric titrations of APols and CylAPols revealed a subtle shift in the degree of ionization, at fixed pH, of the various polymers (Figure S15). The degree of ionization at neutral pH, however, ranks the polymers as follows: A8-50 < C_8-C_0-50 < A8-35, which does not correlate with extraction efficiency. It

seems reasonable to conclude that the cyclic nature of the side groups, rather than the hydrophilic/hydrophobic balance, plays the key role in improving MP extraction.

The relative efficiency of polymers with respect to MP extraction varies depending on the protein under consideration. For instance, the amounts of *Hw*BR extracted from *E. coli* membranes with either A8-35 or SMA (2:1) were much lower than that obtained with SMA (3:1), whereas the amounts of YidC-GFP extracted with these three polymers were similar. A8-50 showed also some variability depending on the protein and/or the membrane used. Similarly, DIBMA showed a poor efficiency at extracting both YidC-GFP and BR, whereas it has been reported to be able to extract other MPs.[30,41] In the present series of experiments, the two CyclAPols showed little sensitivity to the nature of the proteins. In addition, an interesting observation is that *Hs*BR is much more stable when extracted with CyclAPols than with SMAs: it retains 80-85% of its native conformation after 6 h at 50°C, *vs*. ~20% in SMAs. How general this effect is and which mechanism underlies it will require further investigations.

Conclusions

In conclusion, we have shown that cyclic hydrophobic moieties improve the copolymer ability to solubilize membranes as compared to linear aliphatic chains. Detergent-free solubilization of *Hs*BR by CyclAPols was as efficient as with SMA (3:1) and the CyclAPol-extracted *Hs*BR was as stable as in A8-35[5] (a stability that SMAs failed to provide). The CyclAPols can also solubilize different MPs from *E. coli* membranes over a short period of incubation (typically 1h) and at low concentration. Recently, CyclAPols have been validated in structural studies of MPs using cryo-EM single particle analysis and electrospray ionization mass spectrometry.[42] Moreover, CyclAPols are compatible with UV-

visible spectroscopic measurements (Figure S8). By ranking the various copolymers according to their detergent-like efficiency, it appears that differences between CyclAPols and classical APols correlate neither with their hydrophobicity nor with chain ionization, and thus likely reflect specific properties of cycloalkane side-chain self-assemblies and/or binding to membranes.

ASSOCIATED CONTENT

Supporting Information. Polymer characterization by ^{1}H, ^{13}C NMR spectroscopy and potentiometric titrations, UV-visible spectra of polymers, SDS-PAGE analysis of YidC-GFP, kinetics of *Hw*BR extraction, photographs of tubes containing polymer-extracted *Hs*BR after ultracentrifugation, size exclusion chromatography profiles, hydrodynamic diameters of *Hs*BR/DMPC proteoliposomes upon addition of polymer solutions, solubilization of pure liposomes by polymers, potentiometric titrations of polymers in the presence of DMPC liposomes.

AUTHOR INFORMATION

Corresponding Author

* Correspondence should be addressed to Christophe Tribet (christophe.tribet@ens.fr) and Manuela Zoonens (manuela.zoonens@ibpc.fr).

Present Addresses

†ICSM, Univ Montpellier, CEA, CNRS, ENSCM, Marcoule, France.

Author Contributions

MZ led the project. AM, BM, FG, CT and MZ designed the experiments. AM synthesized and characterized the CyclAPols with the help of FG. AM and MZ performed the quantification and kinetics of YidC-GFP solubilization. MZ carried out the *Hw*BR extraction experiments. AM and BP assisted by MZ performed the *Hs*BR extraction and stabilization experiments. BM investigated the effects of *Hs*BR/DMPC and *Hs*BR/polymer ratios. CLB performed the SEC analysis. CT performed and analyzed the DLS experiments. MZ and CT wrote the manuscript. All authors have given approval to the final version of the manuscript.

ACKNOWLEDGMENT

We thank Elodie Point for helping in purple membrane preparation, Oana Ilioaia for producing YidC-GFP in *Escherichia coli*, and Jean-Luc Popot for constructive comments on the manuscript. This work was supported by the Centre National de la Recherche Scientifique (CNRS), with specifically an "80PRIME" grant, the University Paris-7 (Université de Paris), and the "Initiative d'Excellence" program from the French State (Grant "DYNAMO", ANR-11-LABX-0011-01).

ABBREVIATIONS

APols, amphipols; CyclAPols, amphipols bearing cycloalkane side groups; DDM, *n*-Dodecyl *β*-D-maltoside; DIBMA, diisobutylene maleic acid copolymer; DLS, dynamic light scattering; GFP, Green Fluorescent Protein; *Hs*BR, bacteriorhodopsin of *Halobacterium salinarum*; *Hw*BR, bacteriorhodopsin of *Haloquadratum walsbyi*; MPs, membrane proteins; PAA, poly(acrylic acid); SEC, size exclusion chromatography; SMAs, styrene maleic acid copolymers.

REFERENCES

(1) Landry, Y.; Gies, J.-P. Drugs and Their Molecular Targets: An Updated Overview. *Fundam. Clin. Pharmacol.* **2008**, *22* (1), 1–18.

(2) Rucevic, M.; Hixson, D.; Josic, D. Mammalian Plasma Membrane Proteins as Potential Biomarkers and Drug Targets. *Electrophoresis* **2011**, *32* (13), 1549–1564.

(3) Tribet, C.; Audebert, R.; Popot, J. L. Amphipols: Polymers That Keep Membrane Proteins Soluble in Aqueous Solutions. *Proc. Natl. Acad. Sci. U.S.A.* **1996**, *93* (26), 15047–15050.

(4) Zoonens, M.; Popot, J.-L. Amphipols for Each Season. *J. Membr. Biol.* **2014**, *247* (9–10), 759–796.

(5) Popot, J.-L. *Membrane Proteins in Aqueous Solutions: From Detergents to Amphipols*; Springer: New York, 2018.

(6) Le Bon, C.; Michon, B.; Popot, J.-L.; Zoonens, M. Amphipathic Environments for Determining the Structure of Membrane Proteins by Single-Particle Electron Cryo-Microscopy. *submitted for publication*.

(7) Champeil, P.; Menguy, T.; Tribet, C.; Popot, J.-L.; Maire, M. le. Interaction of Amphipols with Sarcoplasmic Reticulum Ca^{2+}-ATPase. *J. Biol. Chem.* **2000**, *275* (25), 18623–18637.

(8) Picard, M.; Duval-Terrié, C.; Dé, E.; Champeil, P. Stabilization of membranes upon interaction of amphipathic polymers with membrane proteins. *Protein Sci.* **2004**, *13* (11), 3056–3058.

(9) Ladavière, C.; Toustou, M.; Gulik-Krzywicki, T.; Tribet, C. Slow Reorganization of Small Phosphatidylcholine Vesicles upon Adsorption of Amphiphilic Polymers. *J. Colloid Interface Sci.* **2001**, *241* (1), 178–187.

(10) Vial, F.; Rabhi, S.; Tribet, C. Association of Octyl-Modified Poly(Acrylic Acid) onto Unilamellar Vesicles of Lipids and Kinetics of Vesicle Disruption. *Langmuir* **2005**, *21* (3), 853–862.

(11) Tribet, C.; Vial, F. Flexible Macromolecules Attached to Lipid Bilayers: Impact on Fluidity, Curvature, Permeability and Stability of the Membranes. *Soft Matter* **2008**, *4* (1), 68–81.

(12) Le Bon, C.; Marconnet, A.; Masscheleyn, S.; Popot, J.-L.; Zoonens, M. Folding and Stabilizing Membrane Proteins in Amphipol A8-35. *Methods* **2018**, *147*, 95–105.

(13) Knowles, T. J.; Finka, R.; Smith, C.; Lin, Y.-P.; Dafforn, T.; Overduin, M. Membrane Proteins Solubilized Intact in Lipid Containing Nanoparticles Bounded by Styrene Maleic Acid Copolymer. *J. Am. Chem. Soc.* **2009**, *131* (22), 7484–7485.

(14) Stroud, Z.; Hall, S. C. L.; Dafforn, T. R. Purification of Membrane Proteins Free from Conventional Detergents: SMA, New Polymers, New Opportunities and New Insights. *Methods* **2018**, *147*, 106–117.

(15) Oluwole, A. O.; Klingler, J.; Danielczak, B.; Babalola, J. O.; Vargas, C.; Pabst, G.; Keller, S. Formation of Lipid-Bilayer Nanodiscs by Diisobutylene/Maleic Acid (DIBMA) Copolymer. *Langmuir* **2017**, *33* (50), 14378–14388.

(16) Yasuhara, K.; Arakida, J.; Ravula, T.; Ramadugu, S. K.; Sahoo, B.; Kikuchi, J.-I.; Ramamoorthy, A. Spontaneous Lipid Nanodisc Fomation by Amphiphilic Polymethacrylate Copolymers. *J. Am. Chem. Soc.* **2017**, *139* (51), 18657–18663.

(17) Jamshad, M.; Grimard, V.; Idini, I.; Knowles, T. J.; Dowle, M. R.; Schofield, N.; Sridhar, P.; Lin, Y.; Finka, R.; Wheatley, M.; Thomas, O. R. T.; Palmer, R. E.; Overduin, M.; Govaerts, C.; Ruysschaert, J.-M.; Edler, K. J.; Dafforn, T. R. Structural Analysis of a Nanoparticle Containing a Lipid Bilayer Used for Detergent-Free Extraction of Membrane Proteins. *Nano Res.* **2015**, *8* (3), 774–789.

(18) Autzen, H. E.; Julius, D.; Cheng, Y. Membrane Mimetic Systems in CryoEM: Keeping Membrane Proteins in Their Native Environment. *Curr. Opin. Struct. Biol.* **2019**, *58*, 259–268.
(19) Nagy, J. K.; Kuhn Hoffmann, A.; Keyes, M. H.; Gray, D. N.; Oxenoid, K.; Sanders, C. R. Use of Amphipathic Polymers to Deliver a Membrane Protein to Lipid Bilayers. *FEBS Lett.* **2001**, *501*, 115–120.
(20) Gorzelle, B. M.; Hoffman, A. K.; Keyes, M. H.; Gray, D. N.; Ray, D. G.; Sanders II, C. R. Amphipols Can Support the Activity of a Membrane Enzyme. *J. Am. Chem. Soc.* **2002**, *124*, 11594-11595.
(21) Giusti, F.; Rieger, J.; Catoire, L. J.; Qian, S.; Calabrese, A. N.; Watkinson, T. G.; Casiraghi, M.; Radford, S. E.; Ashcroft, A. E.; Popot, J.-L. Synthesis, Characterization and Applications of a Perdeuterated Amphipol. *J. Membr. Biol.* **2014**, *247* (9), 909–924.
(22) Hovers, J.; Potschies, M.; Polidori, A.; Pucci, B.; Raynal, S.; Bonneté, F.; Serrano-Vega, M. J.; Tate, C. G.; Picot, D.; Pierre, Y.; Popot, J.-L.; Nehmé, R.; Bidet, M.; Mus-Veteau, I.; Bußkamp, H.; Jung, K.-H.; Marx, A.; Timmins, P. A.; Welte, W. A Class of Mild Surfactants That Keep Integral Membrane Proteins Water-Soluble for Functional Studies and Crystallization. *Mol. Membr. Biol.* **2011**, *28* (3), 171–181.
(23) Dörr, J. M.; Scheidelaar, S.; Koorengevel, M. C.; Dominguez, J. J.; Schäfer, M.; van Walree, C. A.; Killian, J. A. The Styrene–Maleic Acid Copolymer: A Versatile Tool in Membrane Research. *Eur. Biophys. J.* **2016**, *45* (1), 3–21.
(24) Korotych, O.; Mondal, J.; Gattás-Asfura, K. M.; Hendricks, J.; Bruce, B. D. Evaluation of Commercially Available Styrene-Co-Maleic Acid Polymers for the Extraction of Membrane Proteins from Spinach Chloroplast Thylakoids. *Eur. Polym. J.* **2019**, *114*, 485–500.
(25) Zoonens, M.; Miroux, B. Expression of Membrane Proteins at the *Escherichia Coli* Membrane for Structural Studies. *Methods Mol. Biol.* **2010**, *601*, 49–66.
(26) Dilworth, M. V.; Piel, M. S.; Bettaney, K. E.; Ma, P.; Luo, J.; Sharples, D.; Poyner, D. R.; Gross, S. R.; Moncoq, K.; Henderson, P. J. F.; Miroux, B.; Bill, R. M. Microbial Expression Systems for Membrane Proteins. *Methods* **2018**, *147*, 3–39.
(27) Orwick-Rydmark, M.; Lovett, J. E.; Graziadei, A.; Lindholm, L.; Hicks, M. R.; Watts, A. Detergent-Free Incorporation of a Seven-Transmembrane Receptor Protein into Nanosized Bilayer Lipodisq Particles for Functional and Biophysical Studies. *Nano Lett.* **2012**, *12*, 4687–4692.
(28) Broecker, J.; Eger, B. T.; Ernst, O. P. Crystallogenesis of Membrane Proteins Mediated by Polymer-Bounded Lipid Nanodiscs. *Structure* **2017**, *25* (2), 384–392.
(29) Oesterhelt, D.; Stoeckenius, W. Rhodopsin-like Protein from the Purple Membrane of *Halobacterium Halobium*. *Nature New Biol.* **1971**, *233*, 149–152.
(30) Oluwole, A. O.; Danielczak, B.; Meister, A.; Babalola, J. O.; Vargas, C.; Keller, S. Solubilization of Membrane Proteins into Functional Lipid-Bilayer Nanodiscs Using a Diisobutylene/Maleic Acid Copolymer. *Angew. Chem. Int. Ed. Engl.* **2017**, *56* (7), 1919–1924.
(31) Kumazaki, K.; Kishimoto, T.; Furukawa, A.; Mori, H.; Tanaka, Y.; Dohmae, N.; Ishitani, R.; Tsukazaki, T.; Nureki, O. Crystal Structure of *Escherichia Coli* YidC, a Membrane Protein Chaperone and Insertase. *Sci. Rep.* **2014**, *4*, 7299.
(32) Hsu, M.-F.; Fu, H.-Y.; Cai, C.-J.; Yi, H.-P.; Yang, C.-S.; Wang, A. H.-J. Structural and Functional Studies of a Newly Grouped *Haloquadratum Walsbyi* Bacteriorhodopsin Reveal the Acid-Resistant Light-Driven Proton Pumping Activity. *J. Biol. Chem.* **2015**, *290* (49), 29567–29577.

(33) Parmar, M. J.; Lousa, C. D. M.; Muench, S. P.; Goldman, A.; Postis, V. L. G. Artificial Membranes for Membrane Protein Purification, Functionality and Structure Studies. *Biochem. Soc. Trans.* **2016**, *44* (3), 877–882.
(34) Váró, G. Analogies between Halorhodopsin and Bacteriorhodopsin. *Biochim. Biophys. Acta* **2000**, *1460* (1), 220–229.
(35) Raetz, C. R.; Dowhan, W. Biosynthesis and Function of Phospholipids in *Escherichia Coli*. *J. Biol. Chem.* **1990**, *265* (3), 1235–1238.
(36) Popot, J.-L.; Althoff, T.; Bagnard, D.; Banères, J.-L.; Bazzacco, P.; Billon-Denis, E.; Catoire, L. J.; Champeil, P.; Charvolin, D.; Cocco, M. J.; Crémel, G.; Dahmane, T.; de la Maza, L. M.; Ebel, C.; Gabel, F.; Giusti, F.; Gohon, Y.; Goormaghtigh, E.; Guittet, E.; Kleinschmidt, J. H.; Kühlbrandt, W.; Le Bon, C.; Martinez, K. L.; Picard, M.; Pucci, B.; Rappaport, F.; Sachs, J. N.; Tribet, C.; van Heijenoort, C.; Wien, F.; Zito, F.; Zoonens, M. Amphipols from A to Z. *Annu. Rev. Biophys.* **2011**, *40*, 379–408.
(37) Sverzhinsky, A.; Qian, S.; Yang, L.; Allaire, M.; Moraes, I.; Ma, D.; Chung, J. W.; Zoonens, M.; Popot, J.-L.; Coulton, J. W. Amphipol-Trapped ExbB–ExbD Membrane Protein Complex from *Escherichia Coli*: A Biochemical and Structural Case Study. *J. Membr. Biol.* **2014**, *247* (9), 1005–1018.
(38) Maiti, S.; Chatterji, P. R. Comparison of the Aggregation Behavior of Di- and Triblock Nonionic Amphiphiles with Linear and Cyclic Hydrophobic Tails. *Langmuir* **1997**, *13* (19), 5011–5015.
(39) Varadaraj, R.; Bock, J.; Zushma, S.; Brons, N. Influence of Hydrocarbon Chain Branching on Interfacial Properties of Sodium Dodecyl Sulfate. *Langmuir* **1992**, *8* (1), 14–17.
(40) Sugiyama, K.; Esumi, K. Micellar Properties of Sodium Cyclododecyl Sulfate in Aqueous Solution. *Langmuir* **1996**, *12* (10), 2613–2615.
(41) Barniol-Xicota, M.; Verhelst, S. H. L. Stable and Functional Rhomboid Proteases in Lipid Nanodiscs by Using Diisobutylene/Maleic Acid Copolymers. *J. Am. Chem. Soc.* **2018**, *140* (44), 14557–14561.
(42) Higgins, A.; Flynn, A.; Marconnet, A.; Postis, V. L. G.; Lippiat, J.; Chung, C.; Ceska, T.; Zoonens, M.; Sobott, F.; Muench, S. P. Cycloalkane-Modified Amphiphilic Polymers for High Resolution Single Particle Cryo-EM and Mass Spectrometry. *in preparation*.

Table Of Contents:

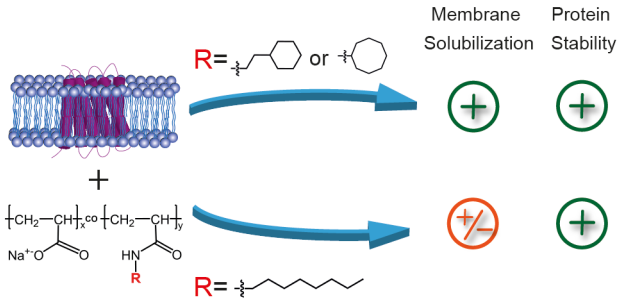

Supporting Information

Solubilization and Stabilization of Membrane Proteins by Cycloalkane-Modified Amphiphilic Polymers

Anaïs Marconnet[1,2], Baptiste Michon[1,2], Christel Le Bon[1,2], Fabrice Giusti[1,2,†]

Christophe Tribet[3,*], Manuela Zoonens[1,2,*]

Affiliations:

[1]Université de Paris, Laboratoire de Biologie Physico-Chimique des Protéines Membranaires, CNRS, UMR 7099, F-75005 Paris

[2]Institut de Biologie Physico-Chimique, Fondation Edmond de Rothschild pour le développement de la recherche Scientifique, F-75005 Paris, France

[3]P.A.S.T.E.U.R., Département de Chimie, École Normale Supérieure, PSL University, Sorbonne Université, CNRS, F-75005 Paris, France

*Correspondence should be addressed to Christophe Tribet (christophe.tribet@ens.fr) or Manuela Zoonens (manuela.zoonens@ibpc.fr)

Supplementary Figures:

1. Chemical composition of C_6-C_2-50 analyzed by ^{1}H and ^{13}C NMR spectroscopy

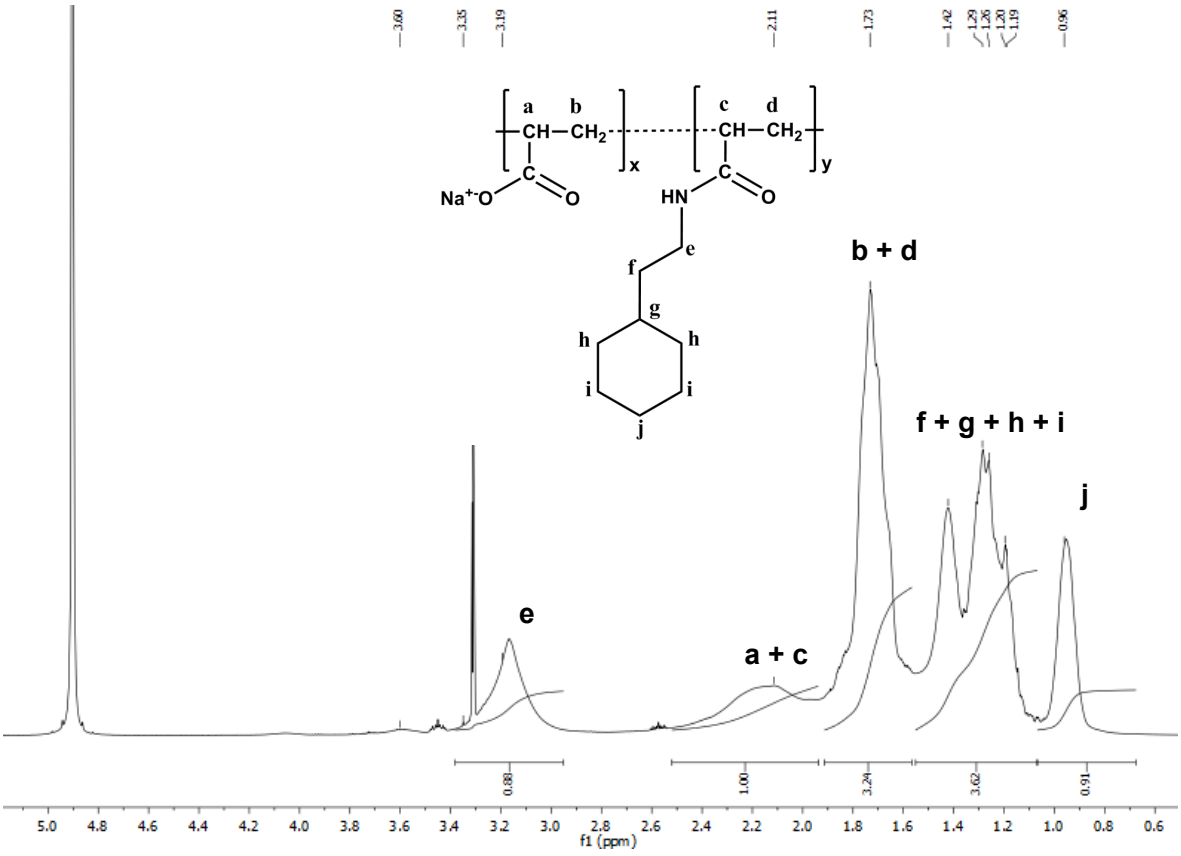

Proton	Number of proton per monomer	δ (ppm)	Theoretical value
e	2	3.16	2*y*
a + c	1 + 1	1.97-2.51	*x* + *y*
b + d	2 + 2	1.56-1.91	2(*x* + *y*)
f + g + h + i	11	0.70-1.55	11*y*
j	2	0.96	2*y*

Figure S1. ^{1}H NMR analysis of C_6-C_2-50 and signal assignments.

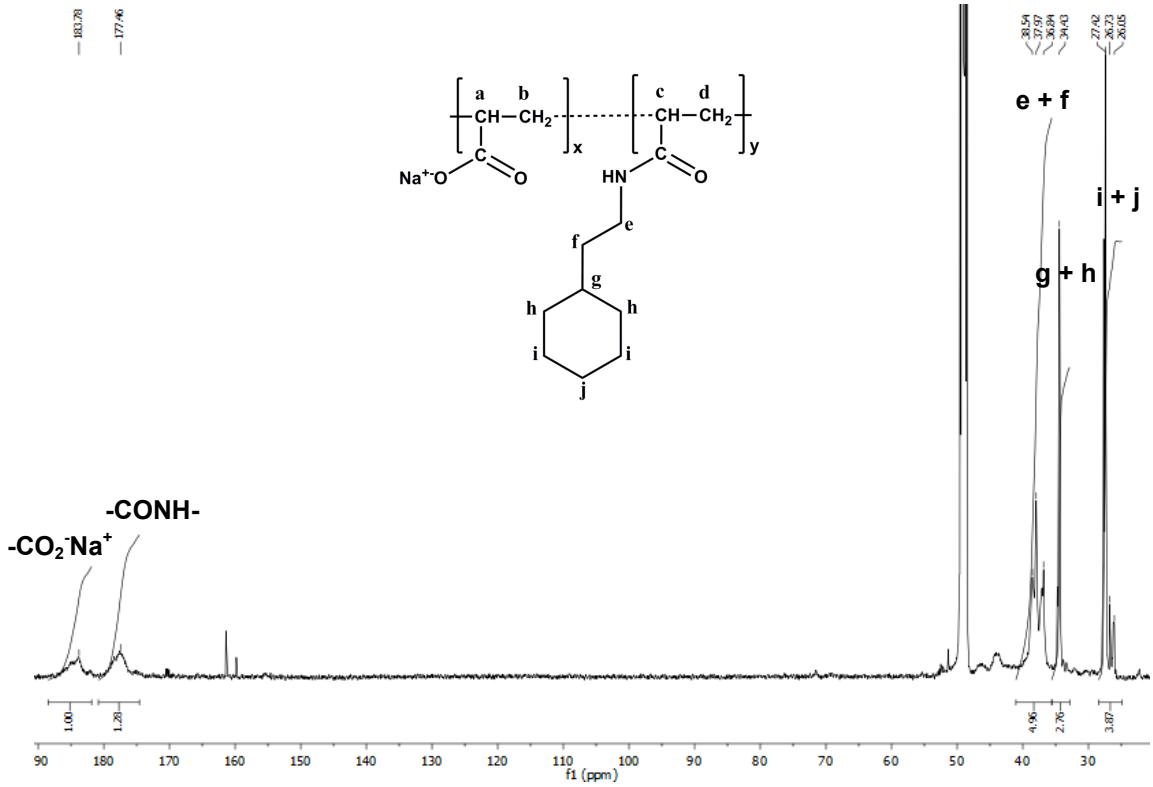

Carbon	Number of carbon per monomer	δ (ppm)	Theoretical value
Free carboxylate	1	183.78	*x*
Carboxamide	1	177.46	*y*
e + f	2	36.17-41.52	2*y*
g + h	3	33.47-35.52	3*y*
i + j	3	26.63-28.38	3*y*

Figure S2. ^{13}C NMR analysis of C_6-C_2-50 and signal assignments.

2. Chemical composition of C_8-C_0-50 analyzed by ^1H and ^{13}C NMR spectroscopy

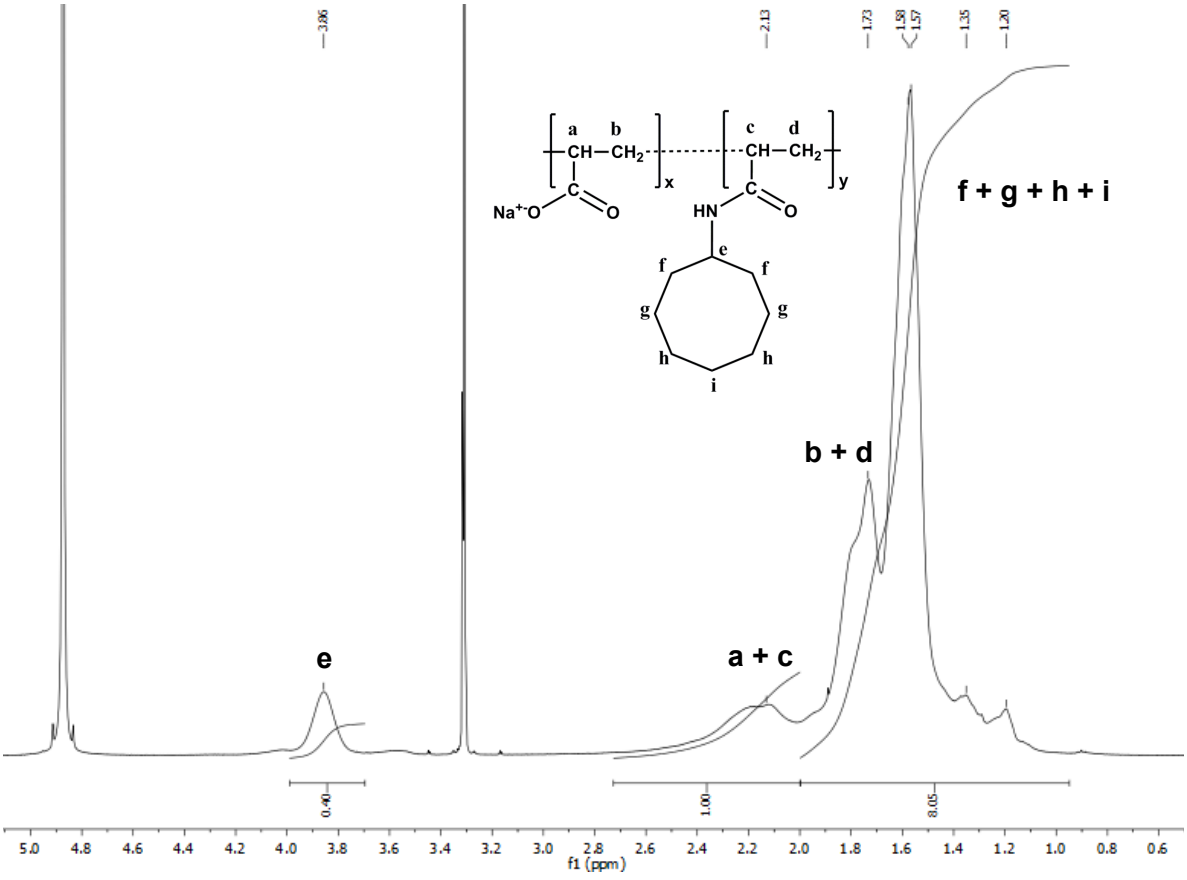

Proton	Number of proton per monomer	δ (ppm)	Theoretical value
e	1	3.86	y
a + c	1 + 1	2.00-2.60	$x + y$
b + d	2 + 2	1.70-2.0	$2(x + y)$
f + g + h + i	14	1.05-1.70	$14y$

Figure S3. ^1H NMR analysis of C_8-C_0-50 and signal assignments.

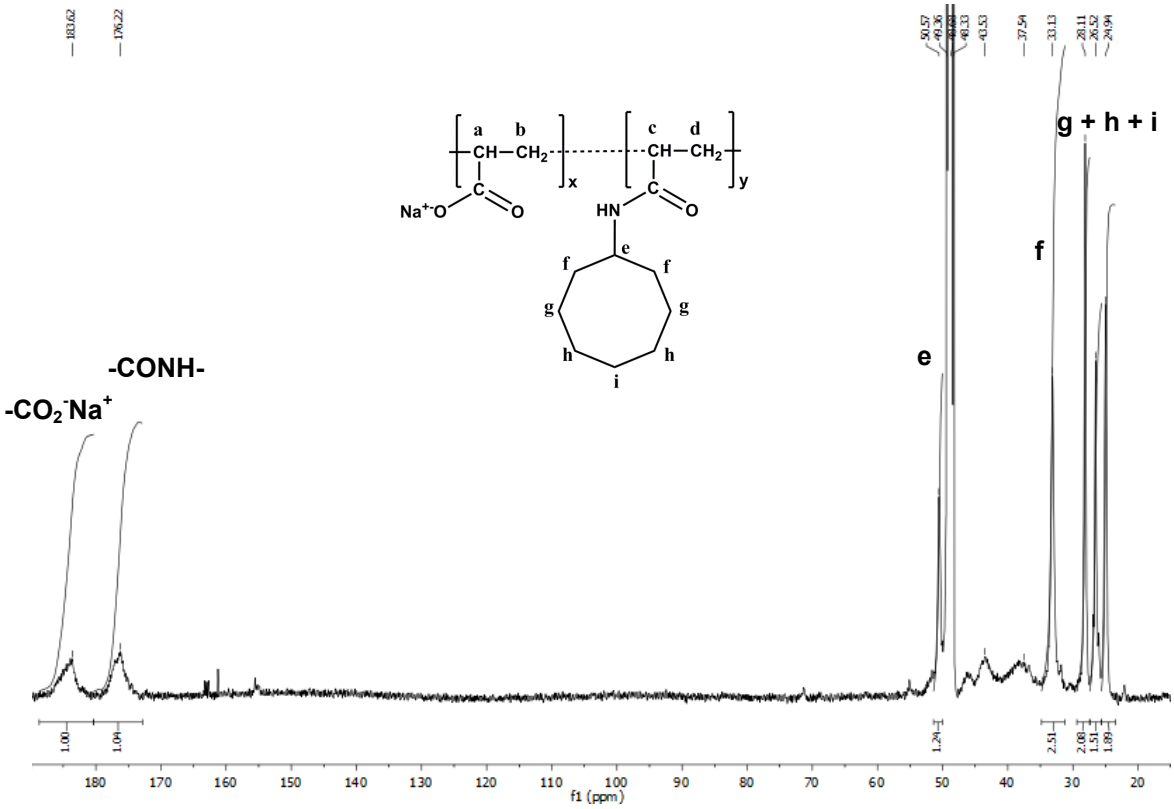

Carbon	Number of carbon per monomer	δ (ppm)	Theoretical value
Free carboxylate	1	183.62	*x*
Carboxamide	1	176.22	*y*
e	1	50.57	*y*
f	2	33.13	2*y*
g + h + i	5	24.94-29.70	5*y*

Figure S4. ^{13}C NMR analysis of C_8-C_0-50 and signal assignments.

3. Chemical composition of A8-50 analyzed by ^{1}H and ^{13}C NMR spectroscopy

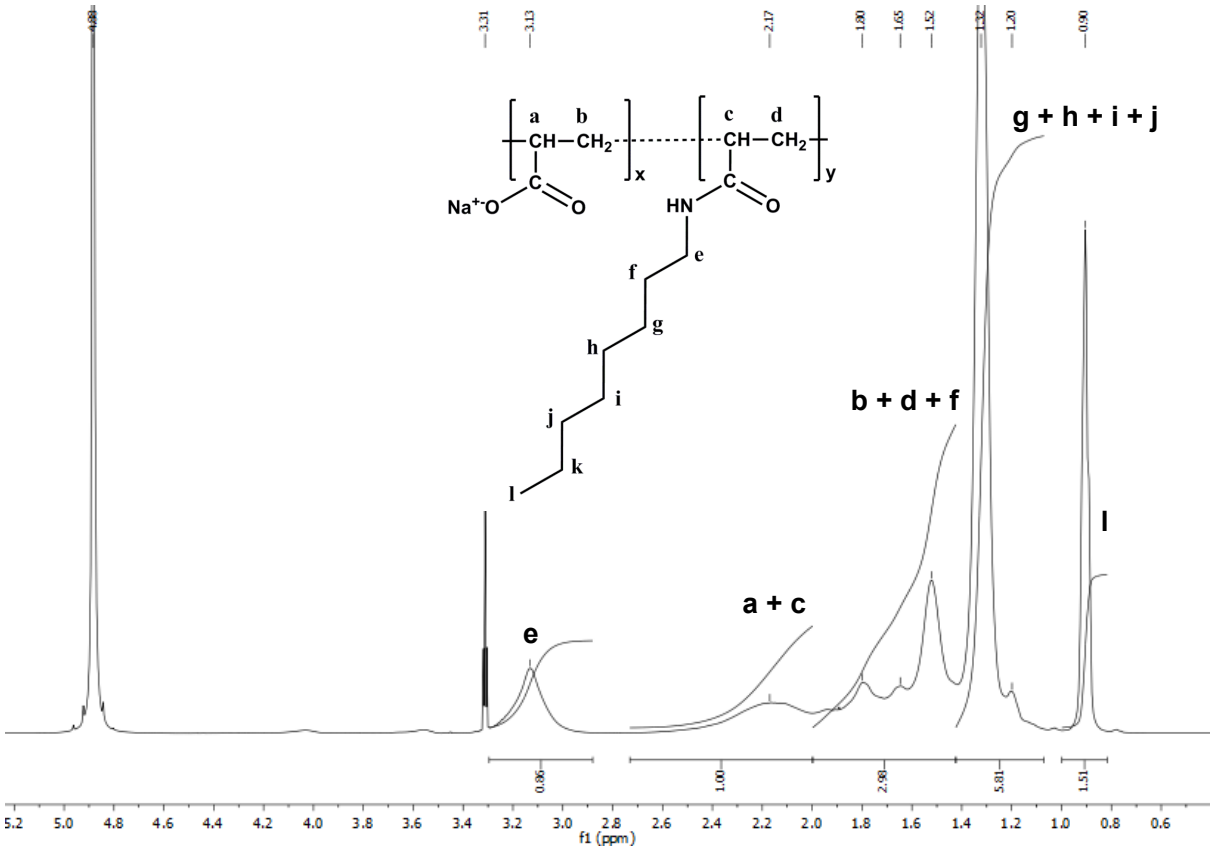

Proton	Number of proton per monomer	δ (ppm)	Theoretical value
e	2	2.86-3.30	2*y*
a + c	1 + 1	2.00-2.55	*x* + *y*
b + d + f	2 + 4	1.43-1.98	2(*x* + 2*y*)
g + h + i + j + k	10	1.07-1.41	10*y*
l	3	0.80-0.98	3*y*

Figure S5. ^{1}H NMR analysis of A8-50 and signal assignments.

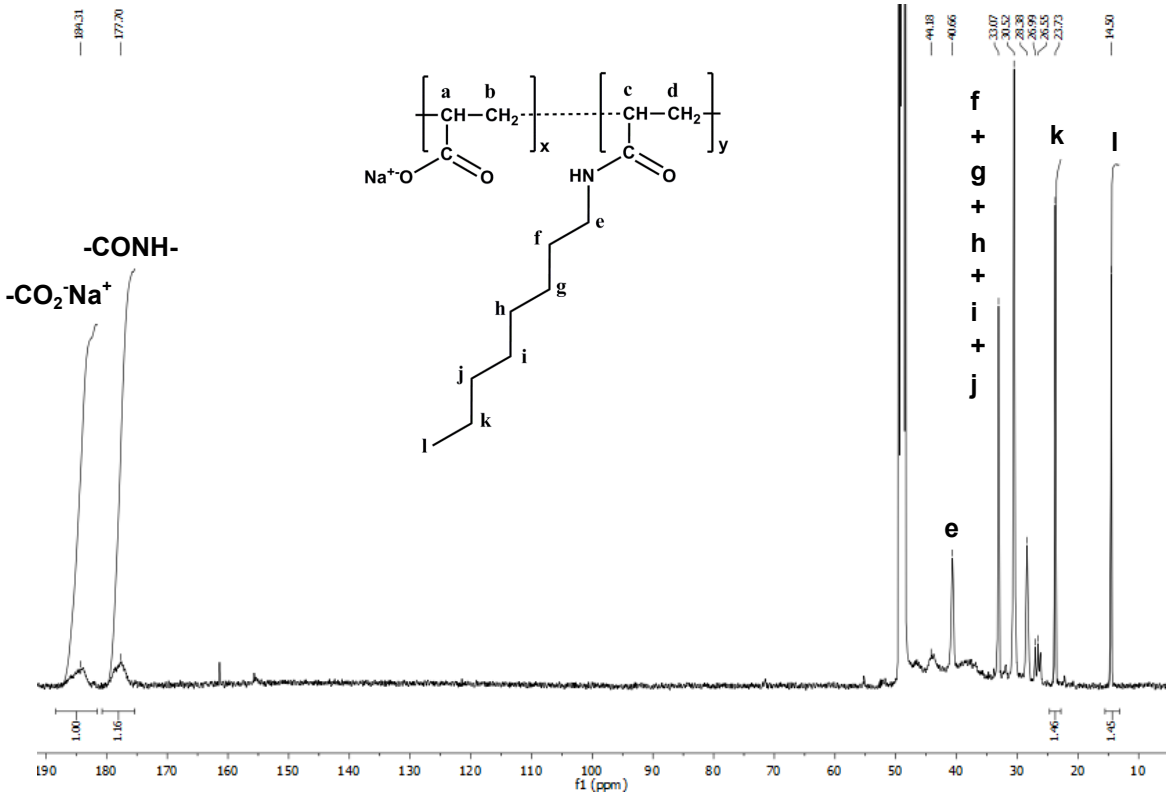

Carbon	Number of carbon per monomer	δ (ppm)	Theoretical value
Free carboxylate	1	184.31	*x*
Carboxamide	1	177.70	*y*
e	1	40.66	*y*
f + g + h + i + j	5	28.38 – 33.07	5*y*
k	1	23.73	*y*
l	1	14.50	*y*

Figure S6. ^{13}C NMR analysis of A8-50 and signal assignments.

4. Potentiometric titrations of polymers in H_2O/Ethanol

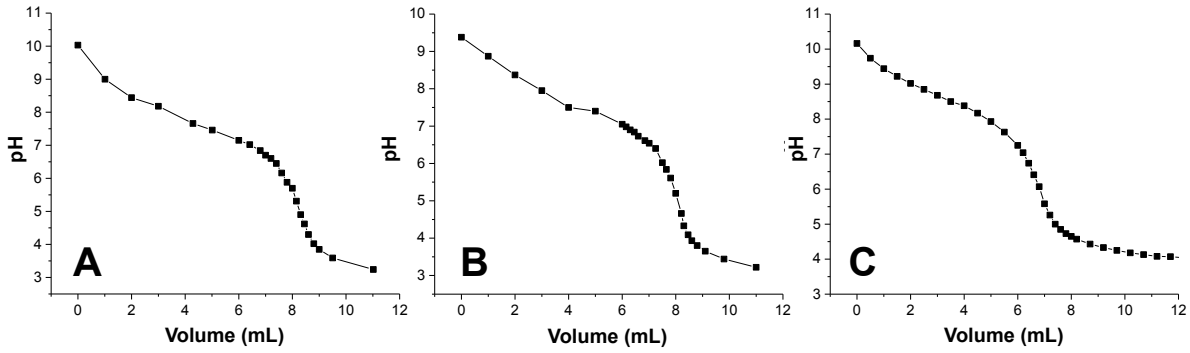

Figure S7. Acid-base titrations of polymers. The titrations of free carboxylate groups of C_6-C_2-50 (A), C_8-C_0-50 (B), and A8-50 (C) were performed at 20 °C in a mixture of water/ethanol (80:20, v/v).

5. UV-visible compatibility of CyclAPols

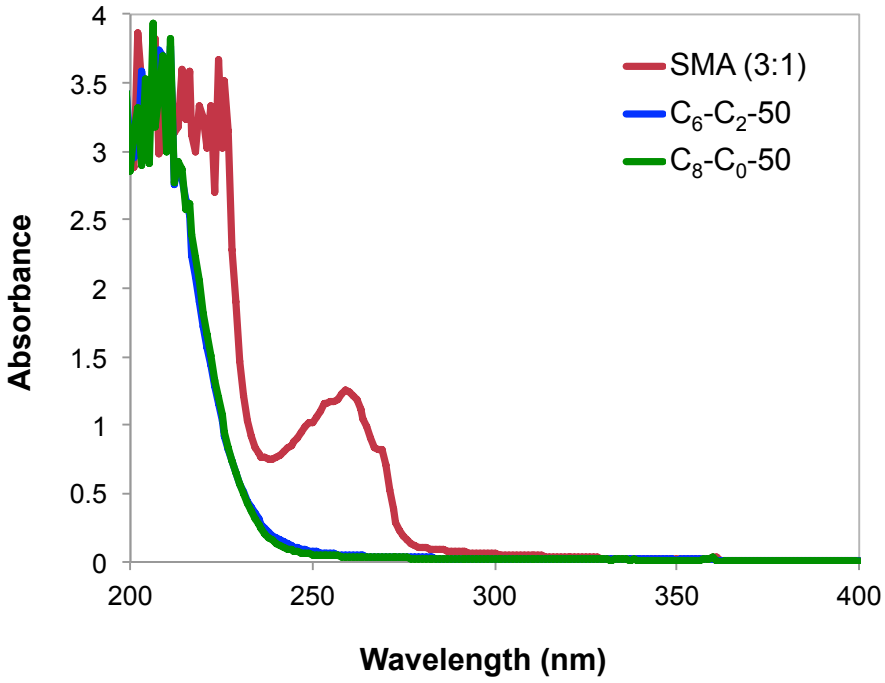

Figure S8. UV-visible spectra of copolymers used in the study. Solutions of polymers were prepared at 1 mg/mL in deionized water. Spectra were recorded using a 10-mm path length cuvette.

6. SDS-PAGE analysis of YidC-GFP extracted from the plasma membrane of *E. coli*

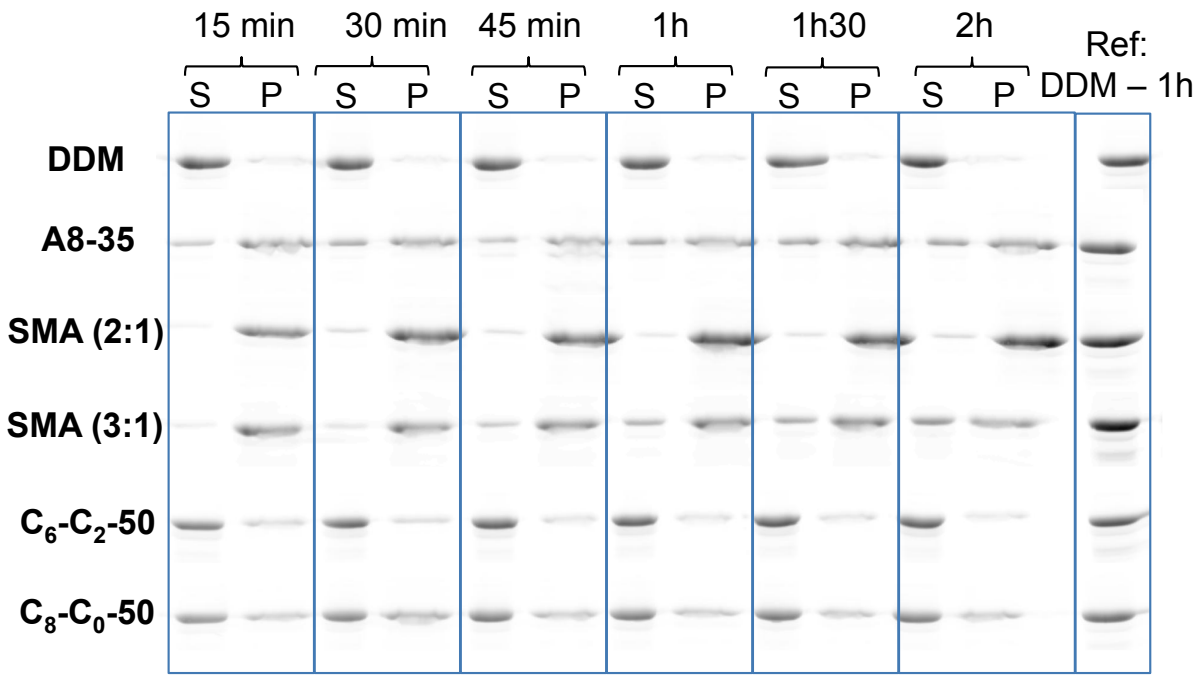

Figure S9. SDS-PAGE analysis of YidC-GFP extracted from *E. coli* membranes using polymers. Over 2-h incubation, aliquots were taken off from samples and centrifuged (10 min. at 250,000 ×*g*). Supernatants (S) and pellets (P) were loaded on 12-% acrylamide gels. After migration, the band of YidC-GFP was visualized on the gels upon exposition to excitation and emission wavelengths (495 and 519 nm, respectively) revealing the GFP fluorescence at the expected position of YidC-GFP.

7. Kinetics of solubilization of *Haloquadratum walsbyi* BR (*Hw*BR) from either pure or DMPC-fused plasma membrane of *E. coli*

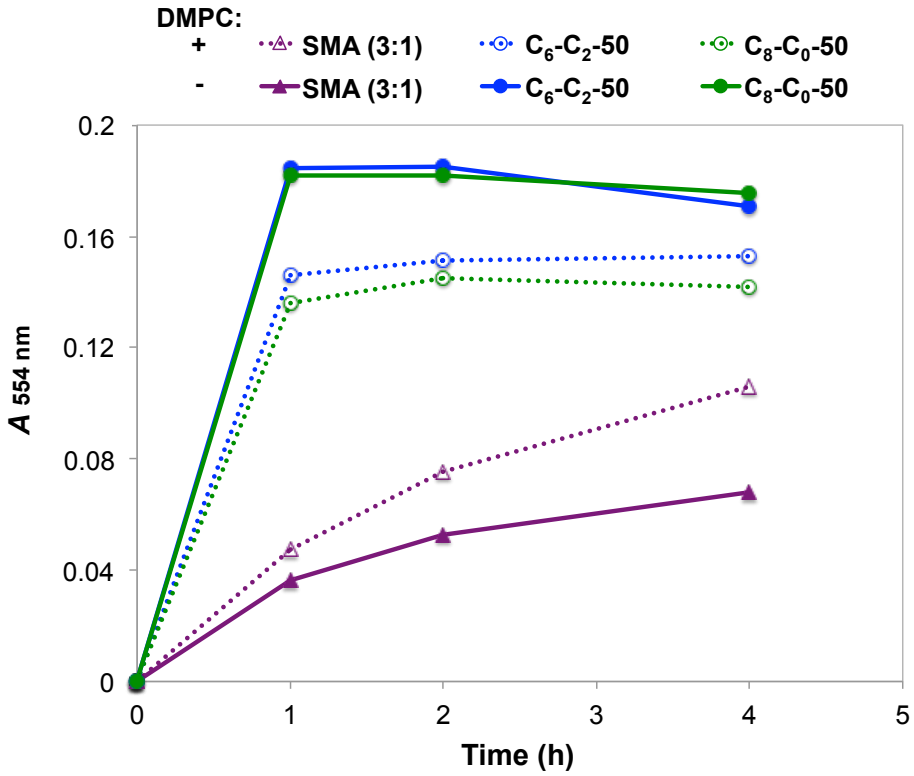

Figure S10. Kinetics of extraction of *Hw*BR from pure membrane or DMPC-fused membrane of *E. coli* with polymers. Extruded DMPC liposomes with a diameter of 100 nm were prepared in buffer 20 mM Tris-HCl, 150 mM NaCl, pH 8.0 and fused by sonication to *E. coli* membranes at a total MP/DMPC ratio of 1:0.5 (w/w). The solubilization was carried out at room temperature in the presence of polymers at 2 g·L^{-1}. Aliquots of each sample were taken off and centrifuged (30 min. at 100,000 ×*g*). The UV-visible spectra of supernatants were measured and the absorbance values at 554 nm plotted as function of time.

8. Comparison of SMA *vs*. DIBMA at solubilizing *Halobacterium salinarum* BR (*Hs*BR) from the DMPC-fused purple membrane

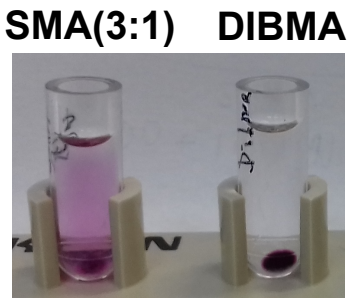

Figure S11. Photographs of samples of the DMPC-fused purple membrane supplemented with either SMA (3:1) or DIBMA after overnight incubation at 25°C, in the dark and

centrifugation (20 min. at 200,000 ×*g*). The *Hs*BR/DMPC ratio was 1:5 (w/w) and the *Hs*BR/polymer ratio used for solubilization was 1:6.25 (w/w).

9. Effect of polymer concentrations on *Hs*BR extraction from the DMPC-fused purple membrane

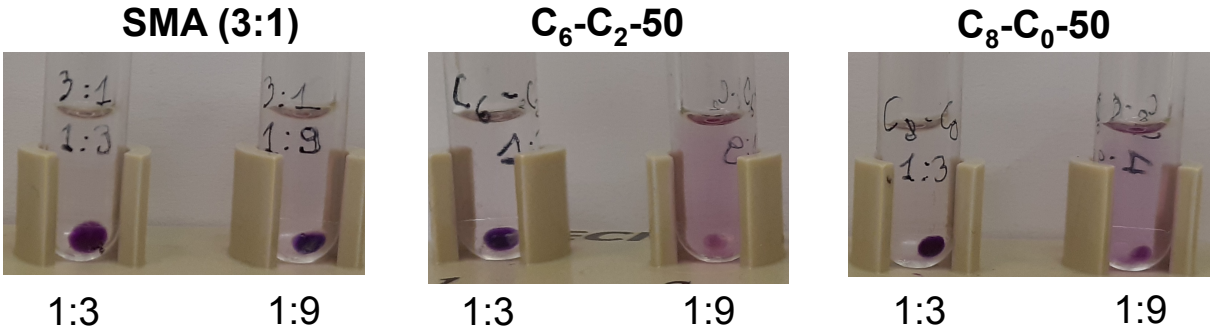

Figure S12. Photographs of samples of the DMPC-fused purple membrane supplemented with polymers after overnight incubation at 25°C, in the dark and centrifugation (20 min. at 200,000 ×*g*). The *Hs*BR/DMPC ratio was 1:5 (w/w) and the *Hs*BR/polymer ratios used for solubilization were either 1:3 or 1:9 (w/w) as indicated.

10. Size exclusion chromatography (SEC) analysis of *Hs*BR/lipid/polymer particles after extraction.

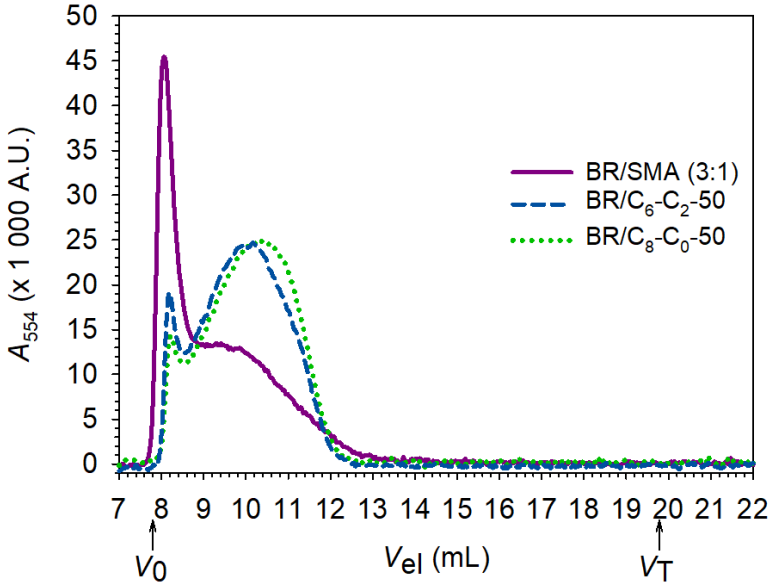

Figure S13. SEC profiles of *Hs*BR/lipid/polymer particles. The DMPC-fused purple membrane was solubilized overnight, in the dark at room temperature with either SMA (3:1), C_6-C_2-50, or C_8-C_0-50. After centrifugation (20 min at 200,000 ×*g*), each sample was injected onto a Superose 12 10/300 GL column connected to an Äkta purifier-10 system. The sample

and elution buffers contained 20 mM sodium phosphate, 100 mM NaCl, pH 7.0. V_0 and V_T stand for the void volume and total volume, respectively.

11. Evolution over time of the hydrodynamic diameters (D_H) of *Hs*BR/DMPC proteoliposomes upon addition of polymer solutions

	D_H (nm)		
Polymers	**after 2.7 h**	**after 24 h**	
		-	**+ centrifugation**
A8-35	210	202	110
A8-50	153	120	51
SMA (2:1)	170	180	32
SMA (3:1)	220	214	nd
C_6-C_2-50	127	75	30
C_8-C_0-50	206	nd	nd

Table S1. Average hydrodynamic diameters (D_H) as measured by DLS along the kinetics after supplementation of *Hs*BR/DMPC proteoliposomes with a solution of polymer (1:1 v/v). The size measurements, performed at two incubation times, *i.e.* 2.7 h and 24 h (before and after centrifugation), are given with a standard error of +/- 15 nm. The (w/w) ratios of *Hs*BR/DMPC and *Hs*BR/polymer were fixed to 1:5 and 1:12.5, respectively.

12. Solubilization of pure DMPC liposomes in the presence of polymers

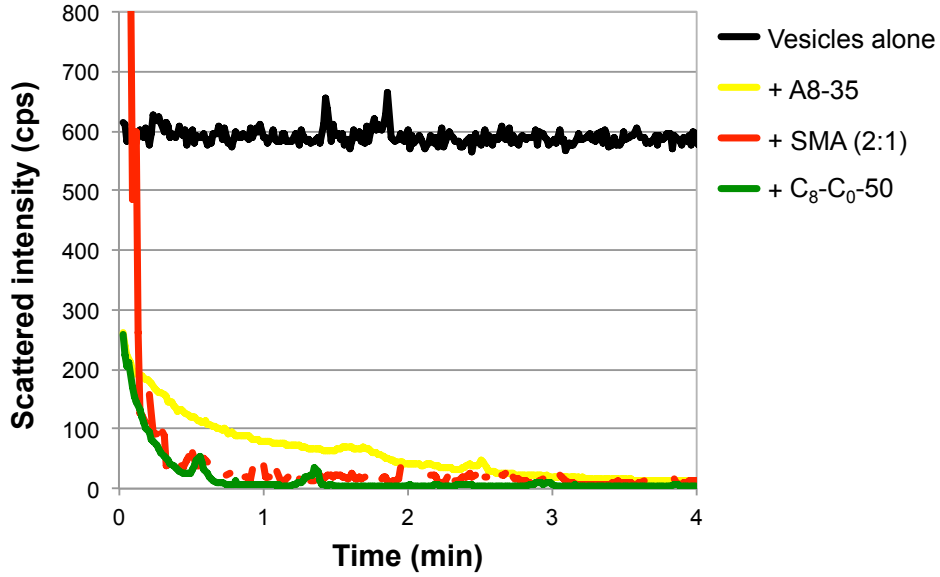

Figure S14. Kinetics of disruption of pure DMPC liposomes upon addition of polymers. Extruded DMPC liposomes with a diameter of 100 nm were prepared in buffer 20 mM sodium phosphate, 100 mM NaCl, pH 7.0. Solubilization was initiated by mixing one volume of liposomes to one volume of polymer solutions to reach a final lipid/polymer (w/w) ratio of 1:1.25. Kinetics were monitored by measuring light scattering intensity, *I*, at 90° angle and 25°C.

13. Potentiometric titrations of polymers in the presence of DMPC liposomes

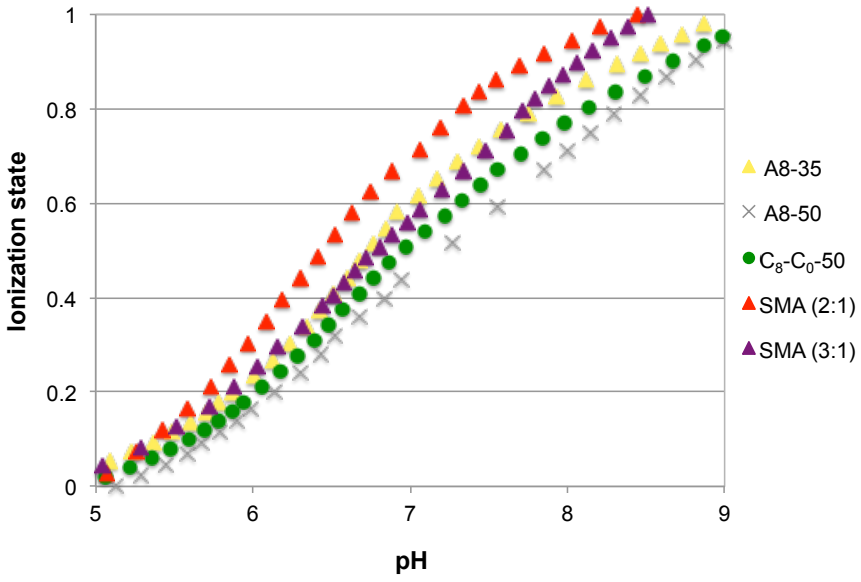

Figure S15. Acid-base titrations of polymer solutions mixed with 100-nm extruded DMPC liposomes. Solutions of polymers were supplemented with 100-nm extruded DMPC

liposomes in deionized water to reach a final polymer/DMPC ratio of 1:10 (w/w). This ratio ensures that neutralized polymer chains (prone to precipitate at low pH in water) can bind to liposomes, thus maintaining their solubility up to the end of titration. The polymers, at a final concentration of 0.25 mg/mL, were titrated with a 0.016-M HCl solution added dropwise in the sample while stirring. The pH values were measured with a nano-electrode (Inlab Nano, Mettler Toledo) at 25 °C after each addition of HCl.